

# On Dynamic Time-Division-Duplex Transmissions for Small-Cell Networks

Ming Ding, *Member, IEEE*, David López-Pérez, *Member, IEEE*, Ruiqi Xue, Athanasios V. Vasilakos, *Senior Member, IEEE*, and Wen Chen, *Senior Member, IEEE*

**Abstract**—Motivated by the promising benefits of dynamic time division duplex (TDD), in this paper, we use a unified framework to investigate both the technical issues of applying dynamic TDD in homogeneous small-cell networks (HomSCNs) and the feasibility of introducing dynamic TDD into heterogeneous networks (HetNets). First, HomSCNs are analyzed, and a small-cell base-station (BS) scheduler that dynamically and independently schedules downlink (DL) and uplink (UL) subframes is presented, such that load balancing between the DL and UL traffic can be achieved. Moreover, the effectiveness of various interlink interference mitigation (ILIM) schemes and their combinations is systematically investigated and compared. Moreover, the interesting possibility of partial interference cancelation (IC) is also explored. Second, based on the proposed schemes, the joint operation of dynamic TDD together with cell range expansion (CRE) and almost blank subframe (ABS) in HetNets is studied. In this regard, scheduling policies in small cells and an algorithm to derive the appropriate macrocell traffic offload and ABS duty cycle under dynamic TDD operation are proposed. Moreover, the full IC and the partial IC schemes are investigated for dynamic TDD in HetNets. The user-equipment (UE) packet throughput performance of the proposed/discussed schemes is benchmarked using system-level simulations.

**Index Terms**—Dynamic time-division duplex (TDD), heterogeneous networks (HetNets), homogeneous networks, interference, small cell.

## I. INTRODUCTION

**I**N recent years, the increase in mobile data traffic has been shown to project an exponential trajectory, and this trend is expected to continue through the next decade [1]. To meet

Manuscript received January 26, 2015; revised November 5, 2015 and December 18, 2015; accepted December 27, 2015. Date of publication January 19, 2016; date of current version November 10, 2016. This work was supported by the National 973 Project under Grant 2012CB316106, by the National 863 Project under Grant 2015AA01A710, by the National Natural Science Foundation of China under Grant 61328101, and by SKL on Mobile Communications under Grant 2013D11. The review of this paper was coordinated by Dr. H. Zhu.

M. Ding is with Data61, Australia (e-mail: Ming.Ding@nicta.com.au).

D. López-Pérez is with Bell Labs Alcatel-Lucent, Dublin, Ireland (e-mail: dr.david.lopez@ieee.org).

R. Xue is with Shanghai Jiao Tong University, Shanghai 200240, China (e-mail: xrq@sjtu.edu.cn).

A. V. Vasilakos is with the Department of Computer Science and Electrical and Space Engineering, Luleå University of Technology, 971 87 Luleå, Sweden (e-mail: th.vasilakos@gmail.com).

W. Chen is with the Shanghai Key Laboratory of Navigation and Location Based Services, Shanghai Jiao Tong University, Shanghai 200240, China, and also with the School of Electronic Engineering and Automation, Guilin University of Electronic Technology, Guilin 541004, China (e-mail: wenchen@sjtu.edu.cn).

Digital Object Identifier 10.1109/TVT.2016.2519520

this formidable traffic demand, telecommunication networks have marched beyond the fourth-generation (4G) realm [2] and begun to explore new advanced technologies [3]. Currently, the Third-Generation Partnership Project (3GPP) is seeing exciting activities in the design of Long-Term Evolution (LTE) Release 13 networks [4], the scopes of which include advanced interference cancelation (IC) receivers [5], LTE operations in unlicensed spectrums [6], [7], device-to-device (D2D) communications [8], [9], enhanced radio resource management [10]–[14], etc. However, the most promising approach to rapidly increase network capacity is network densification through the deployment of small cells in heterogeneous networks (HetNets), which takes advantage of extensive spatial reuse [3], [15]–[20].

LTE Release 10 HetNets, i.e., LTE Advanced (LTE-A) HetNets, adopted cell range expansion (CRE) to maximize the benefits of small cells [2], [16]. With CRE, the coverage of a small cell can be artificially increased by instructing user equipments (UEs) to add a positive range expansion bias (REB) to the reference signal receiving power (RSRP) of the small cell. However, the better spatial reuse and improved uplink (UL) connection offered by CRE comes at the expense of a reduced downlink (DL) signal-to-interference-plus-noise ratio (SINR) for the expanded region (ER) UEs, since they no longer connect to the base station (BS) providing the strongest level of signal reception [16]. To alleviate this interference problem, LTE-A HetNets implement time-domain enhanced intercell interference coordination (eICIC) by introducing almost blank subframes (ABSs) [2], [16]. In more detail, in the DL, macrocells schedule ABSs that are subframes in which only common reference signals and the most important cell-specific broadcast information are transmitted, and small cells typically schedule their ER UEs in those DL subframes overlapping with the macrocell ABSs. In this way, the intertier interference from macrocell BSs (MBSs) to ER UEs can be avoided [16].

In addition to HetNets, it is also envisaged that future wireless communication networks, e.g., LTE Release 12–14 networks, will embrace time division duplexing (TDD), which does not require a pair of frequency carriers and holds the possibility of tailoring the amount of DL/UL radio resources to the traffic conditions. In the LTE Release 8–11 networks, seven TDD configurations [21], each associated with a DL-to-UL subframe ratio in a 10-ms transmission frame, are available for semi-static selection at the network side. However, the adopted semi-static selection of TDD configuration in LTE Release 8–11 networks is not able to adapt DL/UL subframe resources

to the fast fluctuations in DL/UL traffic loads. These fluctuations are exacerbated in small cells due to the low number of connected UEs per small cell and the burstiness of their DL and UL traffic demands.

To allow small cells to smartly and independently adapt their communication service to the quick variation of DL/UL traffic demands, a new technology, i.e., dynamic TDD, has drawn much attention in the 3GPP recently [4]. In dynamic TDD, the configuration of TDD DL-to-UL subframe ratio can be dynamically changed on a per-frame basis, i.e., once every 10 ms, in each cell or a cluster of cells. Dynamic TDD can thus provide a tailored configuration of DL/UL subframe resources for each cell or a cluster of cells at the expense of allowing interlink interference, i.e., the DL transmissions of a cell interfere with the UL ones of a neighboring cell and *vice versa*. Note that, although dynamic TDD is a 4G technology, it serves as the predecessor of the full-duplex transmission technology [22], which has been identified as one of the candidate technologies for the fifth-generation (5G) networks. In a full-duplex system, a BS can transmit to and receive from different UEs simultaneously using the same frequency resource. Hence, aside from the self-interference issue at the transceiver, the full-duplex transmission shares a common problem with dynamic TDD, i.e., the interlink interference.

The application of basic dynamic TDD transmissions in homogeneous small-cell networks (HomSCNs) has been investigated in recent works [23], [24]. Gains in terms of wideband (WB) SINR and UE packet throughput (UPT) have been observed. Faster dynamic TDD configuration timescales have also been shown to outperform slower ones. Moreover, in [25], a preliminary analysis based on stochastic geometry for dynamic TDD in HomSCNs is presented, without the consideration of traffic-adaptive DL/UL schedulers. However, the introduction of dynamic TDD into HetNets is not straightforward because it will complicate the existing CRE and ABS operations [26]. An initial study on the feasibility of dynamic TDD in HetNets can be found in [27].

In this paper, motivated by the promising benefits of dynamic TDD, we investigate both the technical issues of applying dynamic TDD in HomSCNs and the feasibility of introducing dynamic TDD into HetNets. This paper extends our previous works in [24] and [27] on dynamic TDD by making the following novel contributions.

1) Extensive efforts have been done to construct a coherent framework with the same design objectives, modeling assumptions, simulation scenarios, and parameters for both HomSCNs and HetNets. In particular, an ideal genie-aided link adaptation (LA) mechanism is used in this paper, i.e., appropriate modulation and coding schemes are chosen according to the perceived SINRs *after* the DL/UL packets are received. Note that some results in our previous work on dynamic TDD in HetNets [27] were lacking of insights because of the simplistic LA mechanism assumed therein. Hence, as a result of the use of a nonideal link adapter, the true performance of dynamic TDD was not fully revealed in [24] and [27], particularly for dynamic TDD in HetNets [27].

- 2) This paper opens a new avenue of research by analyzing the concept of partial IC and its overhead for dynamic TDD. Two new partial IC schemes are proposed to mitigate the DL-to-UL interference in dynamic TDD, i.e., the BS-oriented partial IC scheme and the UE-oriented partial IC scheme. Results show that the BS-oriented partial IC scheme is much more effective than the UE-oriented partial IC scheme, and canceling a few interferers is usually good enough to mitigate interlink interference.
- 3) The dynamic TDD algorithms in this paper have been redefined compared with those in our previous works [24], [27], such that the algorithms for HomSCNs can be smoothly extended to work in a HetNet scenario. This is important for practical implementation since operators can work with the same hardware/software in different scenarios just with minimal upgrades and no drastic changes.
- 4) In this paper, unlike [24], multiple-input–multiple-output (MIMO) transmissions have also been considered for the UL, which has an impact on the results due to their larger capacity and, thus, shorter time for file transmission. Moreover, MIMO presents challenges on the appropriated switch between single-stream transmissions and multistream transmissions.
- 5) As a result of the above bulletins, all the experiments have been reconducted in this paper, so that an intriguing comparison between dynamic TDD in HomSCNs and HetNets can be performed to shed new light on dynamic TDD operations.

The remainder of this paper is organized as follows. In Section II, the scenarios to analyze the dynamic TDD performance for both HomSCNs and HetNets are introduced. In Sections III and IV, the focus is on dynamic TDD operation in HomSCNs and HetNets, respectively. In Section V, our system-level simulator and the 3GPP simulation parameters in our experiments are presented. In Sections VI and VII, benchmarked network configurations are depicted, and simulation results for a HomSCN and a HetNet are presented and discussed, respectively. Finally, a fair performance comparison between dynamic TDD in HomSCNs and HetNets is conducted in Section VIII, followed by the concluding remarks in Section IX.

## II. NETWORK SCENARIO

During the study of dynamic TDD in the 3GPP [26], a total of eight deployment scenarios were considered for investigation. The 3GPP prioritized Scenario 3 for further analysis [4], and the study of Scenario 6 was left open for further discussion. The definition of Scenarios 3 and 6 is as follows.

- Scenario 3: multiple outdoor picocells deployed on the same carrier frequency, where outdoor picocells can dynamically adjust TDD configurations;
- Scenario 6: multiple outdoor macrocells and multiple picocells deployed on the same carrier frequency, where all macrocells have the same TDD configuration and outdoor picocells can adjust TDD configurations.

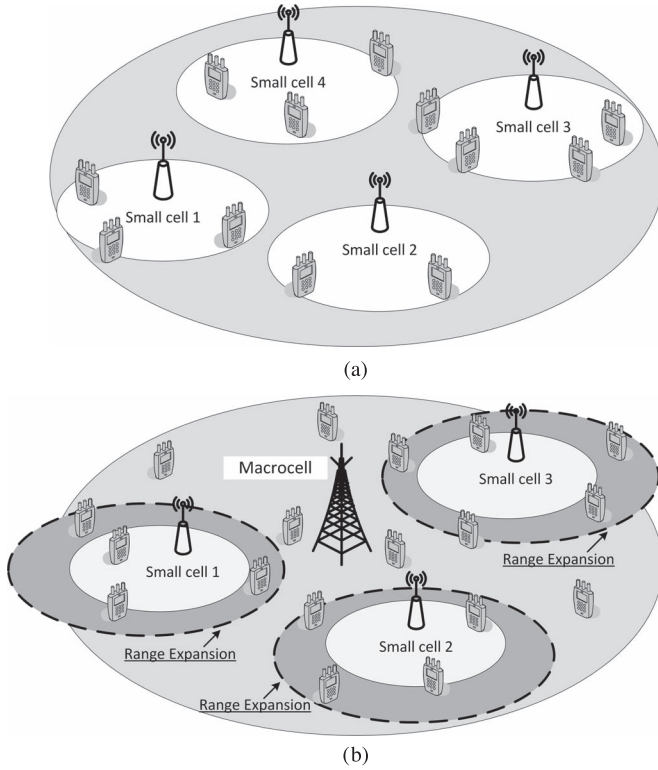


Fig. 1. Dynamic TDD scenarios. (a) Scenario 3: HomSCN. (b) Scenario 6: Heterogeneous small-cell network.

In this paper, we focus on Scenarios 3 and 6, which are shown in Fig. 1.

With regard to notations, in Fig. 1, the  $m$ th MBS, the  $n$ th small-cell BS (SBS), and the  $q$ th UE are denoted  $b(m)$ ,  $m \in \{1, \dots, M\}$ ,  $c(n)$ ,  $n \in \{1, \dots, N\}$ , and  $u(q)$ ,  $q \in \{1, \dots, Q\}$ , respectively. Moreover, the DL average traffic arriving rate (DATAR), the UL average traffic arriving rate (UATAR), the DL instantaneous data buffer (DIDB), and the UL instantaneous data buffer (UIDB) of UE  $u(q)$  are denoted  $\lambda^{\text{DL}}(q)$ ,  $\lambda^{\text{UL}}(q)$ ,  $\omega^{\text{DL}}(q)$ , and  $\omega^{\text{UL}}(q)$ , respectively.

To determine UE cell association, two measures, RSRP and WB DL SINR, have been widely used in practical systems, e.g., LTE-A networks [2]. The RSRP in dBm scale and WB DL SINR in decibel scale measured at UE  $u(q)$  associated with MBS  $b(m)$  are denoted  $\mu_{m,q}^M$  and  $\gamma_{m,q}^M$ , respectively. The counterpart measures for SBS  $c(n)$  are denoted  $\mu_{n,q}^S$  and  $\gamma_{n,q}^S$ , respectively. Based on the best RSRP criterion of UE association, we assume the following.

- The set of macrocell UEs served by MBS  $b(m)$  is denoted by  $U_m^M = \{u(q_{m,k}^M)\}$ ,  $k \in \{1, \dots, K_1(m)\}$ , where  $Q_m^M = \{q_{m,k}^M\}$  is the set of indexes of such macrocell UEs, and  $K_1(m)$  is its cardinality. Note that the original set of macrocell UEs served by MBS  $b(m)$  without the CRE operation is denoted by  $U_m^{M*}$ , and its cardinality is  $K_1^*(m)$ .
- Without CRE in the small cells, the set of small-cell UEs served by SBS  $c(n)$  is denoted by  $U_n^S = \{u(q_{n,k}^S)\}$ ,  $k \in \{1, \dots, K_2(n)\}$ , where  $Q_n^S = \{q_{n,k}^S\}$  is the set of indexes of original small-cell UEs, and  $K_2(n)$  is its cardinality.

- After the CRE operation, some macrocell UEs will migrate to small cells, leading to traffic offloading from the macrocell tier to the small-cell tier. Then, the set of offloaded macrocell UEs to SBS  $c(n)$  is denoted  $U_n^{M2S} = \{u(r_{n,k}^S)\}$ ,  $k \in \{1, \dots, K_3(n)\}$ , where  $R_n^{M2S} = \{r_{n,k}^S\}$  is the set of indexes of such ER UEs, and  $K_3(n)$  is its cardinality.

For clarity, the notation of variables related to UE  $u(q)$  is summarized in Table I. In dynamic TDD, the subframes that can be either DL or UL ones are referred to as dynamic TDD subframes. For those dynamic TDD subframes converted to DL ones or UL ones, we refer to them as dynamic DL subframes and dynamic UL subframes, respectively.

It is important to note that, in the following, we propose dynamic TDD schemes based on several coherent optimization objectives, which are summarized here for the sake of clarity:

- **Objective 1:** to minimize the difference between the DL and the UL *average* traffic demand densities in each small cell;
- **Objective 2:** to minimize the difference between the DL and the UL *instantaneous* traffic demand densities in each small cell;
- **Objective 3:** to minimize the *average* traffic demand density for the macrocell and the small-cell tiers.

### III. DYNAMIC TIME DIVISION DUPLEX OPERATION IN HOMOGENEOUS SMALL-CELL NETWORKS

In Scenario 3, as shown in Fig. 1(a), multiple outdoor pico-cells deployed on the same carrier frequency can independently adapt their DL and UL subframe usage to the quick variation of the DL/UL traffic demands. The following two design aspects are fundamental to allow such dynamic TDD operation in each small cell:

- algorithms to decide the appropriate TDD configuration; to be more specific, how many subframes should be scheduled as DL or UL subframes in every  $T$  subframes;
- interference mitigation schemes to deal with the new interlink interference, i.e., the DL transmissions of small cells interfering with the UL transmissions of neighboring ones and *vice versa*.

Here, we present algorithms and schemes to realize these two design aspects.

#### A. Dynamic DL/UL Subframe Splitting

In the following, we present an algorithm that runs independently in each small cell and decides the appropriate TDD configuration for each small cell. Two cases are distinguished, whether the small cell has active traffic or not.

First, the case in which there is no instantaneous DL or UL traffic at the small cell is considered. In other words, the small cell  $c(n)$  is completely idle, i.e.,  $\omega^{\text{DL}}(q_{n,k}^S) = 0$  and  $\omega^{\text{UL}}(q_{n,k}^S) = 0 \forall q_{n,k}^S \in Q_n^S$ . Then, we propose that the number of dynamic UL subframes should be set to a statistically optimal value that meets the upcoming traffic and achieves **Objective 1**, i.e., to minimize the difference between the DL

TABLE I  
NOTATION OF VARIABLES

Items	MBS $b(m)$	SBS $c(n)$ (w/o CRE)	SBS $c(n)$ (w/ CRE)
Serving UEs	$U_m^M = \{u(q_{m,k}^M)\}$	$U_n^S = \{u(q_{n,k}^S)\}$	/
ER UEs	/	/	$U_n^{M2S} = \{u(r_{n,k}^S)\}$
UE indices	$Q_m^M = \{q_{m,k}^M\}$	$Q_n^S = \{q_{n,k}^S\}$	$R_n^{M2S} = \{r_{n,k}^S\}$
UE number	$K_1(m)$	$K_2(n)$	$K_3(n)$
RSRP	$\mu_{m,q_{m,k}^M}^M$	$\mu_{n,q_{n,k}^S}^S$	$\mu_{n,r_{n,k}^S}^S$
WB DL SINR	$\gamma_{m,q_{m,k}^M}^M$	$\gamma_{n,q_{n,k}^S}^S$	$\gamma_{n,r_{n,k}^S}^S$
DATAR	$\lambda^{DL}(q_{m,k}^M)$	$\lambda^{DL}(q_{n,k}^S)$	$\lambda^{DL}(r_{n,k}^S)$
UATAR	$\lambda^{UL}(q_{m,k}^M)$	$\lambda^{UL}(q_{n,k}^S)$	$\lambda^{UL}(r_{n,k}^S)$
DIDB	$\omega^{DL}(q_{m,k}^M)$	$\omega^{DL}(q_{n,k}^S)$	$\omega^{DL}(r_{n,k}^S)$
UIDB	$\omega^{UL}(q_{m,k}^M)$	$\omega^{UL}(q_{n,k}^S)$	$\omega^{UL}(r_{n,k}^S)$

and the UL average traffic demand densities in each small cell, where the DL (UL) average traffic demand density is defined as the sum of UEs' DL (UL) average traffic arriving rates over the quantity of the corresponding subframe resources in  $T$  subframes.

Formally, the average traffic demand densities in small cell  $c(n)$  in the DL and the UL are defined, respectively, as follows:

$$d_n^{S,DL}(t) = \frac{\sum_{k=1}^{K_2(n)} \lambda^{DL}(q_{n,k}^S)}{T-t} \quad (1)$$

$$d_n^{S,UL}(t) = \frac{\sum_{k=1}^{K_2(n)} \lambda^{UL}(q_{n,k}^S)}{t} \quad (2)$$

where the numerator is the sum of the DATARs(UATARs)  $\lambda^{DL(UL)}(q_{n,k}^S)$  of all UEs connected to small cell  $c(n)$ , and the denominator is the number of DL (UL) subframes in every  $T$  subframes available to transmit in the DL (UL); such number is denoted  $T-t$  for the DL and  $t$  for the UL. The definitions proposed in (1) and (2) make sense because the DATAR and the UATAR measure the average traffic influx into the network for the DL and the UL, respectively.

Then, with respect to **Objective 1**, the statistically optimal number of dynamic TDD UL subframes for small cell  $c(n)$  is selected from

$$t_n^{STAT\_homo} = \arg \min_{t=g(r), r \in \Upsilon^{homo}} \{|d_n^{S,UL}(t) - d_n^{S,DL}(t)|\} \quad (3)$$

where  $\Upsilon^{homo}$  is the set of all available TDD configurations for the considered HomSCN,  $r$  is one specific TDD configuration, and  $g(r) \in [1, T-1]$  extracts the number of UL subframes in  $T$  subframes from TDD configuration  $r$ . In general,  $t_n^{STAT\_homo}$  indicates a reasonable standby state, which tunes each small cell to be prepared for the upcoming traffic.

It is important to note the following.

- $g(r)$  may not be limited to integer values since in practical systems certain special subframes consist of DL symbols, UL symbols, and a transition interval between the DL and

the UL symbols [21]. The proportion of these three parts depends on the specific TDD configuration  $r$ .

- To keep the DL/UL control/reference signal channels always open for the TDD system to function properly, we assume that  $\Upsilon^{homo}$  only contains reasonable TDD configurations with  $g(r) \in [1, T-1]$ . In other words, there are at least one DL and one UL subframe available in every  $T$  subframes. Note that all the 3GPP TDD configurations satisfy the above constraint [21].

In the following, the case in which there is some active DL and/or UL traffic at the small cell is considered. In this case, the optimization objective is changed to **Objective 2**, i.e., to minimize the difference between the DL and the UL instantaneous traffic demand densities in each small cell, where the DL (UL) instantaneous traffic demand density is defined as the sum of UEs' DIDBs(UIDBs) over the quantity of the corresponding subframe resources in  $T$  subframes. This optimization objective ensures that load balancing between the DL and UL transmissions can be dynamically achieved since both the DIDB and UIDB are instantaneous information characterizing the immediate network loads.

Formally and similar to  $d_n^{DL}(t)$  and  $d_n^{UL}(t)$ , the instantaneous traffic demand densities of small cell  $c(n)$  in the DL and the UL are defined, respectively, as follows:

$$\tilde{d}_n^{S,DL}(t) = \frac{\sum_{k=1}^{K_2(n)} \omega^{DL}(q_{n,k}^S)}{T-t} \quad (4)$$

$$\tilde{d}_n^{S,UL}(t) = \frac{\sum_{k=1}^{K_2(n)} \omega^{UL}(q_{n,k}^S)}{t} \quad (5)$$

where the numerator is the sum of the DIDBs (UIDBs)  $\omega^{DL(UL)}(q_{n,k}^S)$  of all UEs connected to small cell  $c(n)$ .

Then and similarly as in (3), with respect to **Objective 2**, the instantaneous optimal number of dynamic TDD UL subframes in  $T$  subframes for small cell  $c(n)$  is selected from

$$t_n^{INST\_homo} = \arg \min_{t=g(r), r \in \Upsilon^{homo}} \{|\tilde{d}_n^{S,UL}(t) - \tilde{d}_n^{S,DL}(t)|\}. \quad (6)$$

In Algorithm 1, we summarize the proposed method to compute the dynamic TDD DL/UL subframe splitting for a given small cell according to its traffic condition in a HomSCN.

---

**Algorithm 1** Selection of the optimal number of instantaneous dynamic TDD UL subframes in a small cell, i.e.,  $t_n^{\text{INST\_homo}}$ , for a HomSCN

---

Compute  $d_n^{S,\text{DL}}(t)$ ,  $d_n^{S,\text{UL}}(t)$ ,  $\tilde{d}_n^{\text{DL}}(t)$ , and  $\tilde{d}_n^{\text{UL}}(t)$ , using (1) and (2), (4), and (5), respectively.

Select  $t_n^{\text{INST\_homo}}$  using the following procedure.

**if**  $\omega^{\text{UL}}(q_{n,k}^S) = 0, \forall q_{n,k}^S \in Q_n^S$  **and**  $\omega^{\text{DL}}(q_{n,k}^S) = 0, \forall q_{n,k}^S \in Q_n^S$

**then**

    Obtain  $t_n^{\text{INST\_homo}} = t_n^{\text{STAT\_homo}}$  using (3).

**else**

    Obtain  $t_n^{\text{INST\_homo}}$  using (6).

**end if**

---

### B. Interlink Interference Mitigation Schemes

It can be expected that the dynamic TDD DL/UL subframe splitting described in Section III-A enables traffic-adaptive scheduling, i.e., more UL subframes will be diverted to DL transmissions when the DL traffic demand density in a small cell is higher than the UL one and *vice versa*. However, dynamic TDD DL/UL subframe splitting gives rise to a new type of interference, which is the interlink interference between DL and UL transmissions resulted from nonuniform TDD subframe configurations among adjacent cells. This kind of interlink interference is particularly severe in the DL-to-UL case because 1) a BS-to-BS path loss is normally much smaller than a UE-to-BS one, and 2) the DL signal from a high-power BS may easily overwhelm a low-power UE's UL signal intended for another BS.

Various interlink interference mitigation (ILIM) schemes can be applied to address this DL-to-UL interference problem, such as cell clustering (CC) [26], DL power reduction (DLPR) [28], UL power boosting (ULPB) [29], IC [24], and their combinations. For brevity, the DLPR scheme will not be considered hereafter, due to its known poor performance, i.e., the DL performance is heavily scarified in exchange of decreasing the DL-to-UL interference and improving the UL performance [24]. More advanced techniques such as the machine learning techniques [30], [31] can also be applied in dynamic TDD to tackle the DL-to-UL interference problem. For example, the machine learning techniques could be invoked at BSs to determine the right frequency and power allocation in view of buffer status and interlink interference conditions. However, the potential performance gains come at the cost of overhead and complexity. We will consider such advanced ILIM schemes in our future work with emphasis on performance improvement and convergence issues.

In the following, we discuss the CC scheme, the ULPB scheme, and the IC scheme, whose performance will be com-

pared later. Note that these ILIM schemes can be classified into two strategies to cope with the DL-to-UL interference: 1) to weaken the DL interference or 2) to strengthen the UL signal. The CC scheme and the IC scheme belong to the first strategy, whereas the ULPB scheme represents the second strategy.

1) *Cell Clustering*: The CC scheme semi-statically organizes the small cells into cell clusters based on metrics such as coupling loss  $\text{PL}^{\text{CC}}$ , i.e., the path loss between SBSs [26]. Then, the dynamic TDD configuration is conducted on a per-cluster basis, rather than on a per-cell basis. In other words, the TDD configuration of all the small cells in a cell cluster is the same; thus, the interlink interference is eliminated within the cell cluster. In this case, negotiation and coordination of TDD configurations within cell clusters are required through intercell communications over backhaul links or the air interface. A simple method to perform dynamic TDD DL/UL subframe splitting for a given cell cluster is to sum the cell specific  $\tilde{d}_n^{S,\text{DL}}(t)$  and  $\tilde{d}_n^{S,\text{UL}}(t)$ , and  $d_n^{S,\text{DL}}(t)$  and  $d_n^{S,\text{UL}}(t)$  over the small cells in such cell cluster, and proceed accordingly with Algorithm 1 for each cell cluster. Note that a more dynamic CC scheme considering joint optimization of DL/UL scheduling among multiple small cells might be possible. However, it is out of the scope of this paper. Here, we only consider the semi-static CC scheme that allows distributed operations among small cell clusters [26].

2) *Power Control*: The power control strategy considered here is based on ULPB [29]. The ULPB scheme increases the amount of transmit power used at the UEs compared with the traditional fractional path-loss compensation power control [21]. This UL power boost helps to combat the DL-to-UL interference coming from neighboring small cells. The implementation of the ULPB scheme is relatively simple, e.g., a fixed power offset  $\Delta P^{\text{UL}}$  can be configured on top of the UL power level.

3) *Interference Cancellation*: In this paper, the IC scheme refers to the DL-to-UL IC and not to the UL-to-DL IC because it is technically more feasible to assume that BSs are capable of exchanging information and canceling interlink interference coming from neighboring BSs. In contrast, the assumption of UEs performing UL-to-DL IC with regard to other peer UEs would seem to be too farfetched and thus impractical (it is unlikely that UEs can exchange information). In theory, the IC scheme should provide the best ILIM for the UL compared with the CC and the ULPB schemes, but requires good backhaul connections for the exchange of intercell information on DL transmission assumptions, such as resource allocation, modulation and coding scheme, etc. Moreover, strong signal processing units are required in the BSs to detect, reconstruct, and cancel the DL interference for UL.

To reduce the complexity and cost of the IC scheme, partial IC schemes can be further considered. To be more specific, in the following, we propose a UE-oriented IC (UOIC) scheme and a BS-oriented IC (BOIC) scheme.

In the UOIC scheme, only cell-edge UEs will be granted the use of IC to mitigate the DL-to-UL interference. Here, cell-edge UEs can be identified as those UEs, which have at least one RSRP associated with a neighboring BS that is larger than the RSRP associated with the serving BS by a bias of  $x_1$  dB.

Formally, for a UE  $u(q_{n,k}^S)$ ,  $q_{n,k}^S \in Q_n^S$ , it is a cell-edge UE entitled for IC if the following condition is valid:

$$\exists \mu_{m,q_{n,k}^S}^S > \mu_{n,q_{n,k}^S}^S - x_1, \quad m \neq n. \quad (7)$$

In the BOIC scheme, only DL interference from neighboring BSs, whose path losses to the serving BS are less than  $x_2$  dB, are canceled. Formally, for an SBS  $c(n)$ , a neighboring SBS  $c(m)$  satisfying the following condition will be treated in the IC process:

$$PL_{m,n}^{S2S} < x_2, \quad m \neq n \quad (8)$$

where  $PL_{m,n}^{S2S}$  is the path loss from SBS  $c(m)$  to SBS  $c(n)$  in decibel scale.

Note that, in both partial IC schemes, the selected UE set and the selected BS set for the IC operations are cell specific.

#### IV. SMALL-CELL DYNAMIC TIME DIVISION DUPLEX OPERATION IN HETNETS

In Scenario 6 shown in Fig. 1(b), it is assumed that multiple outdoor macrocells and multiple picocells are deployed on the same carrier frequency, and that all macrocells have the same TDD configuration, whereas outdoor picocells can adjust their TDD configurations. This is a logical assumption since macrocell traffic dynamics are usually averaged out due to the fairly large number of macrocell UEs per macrocell site. Moreover, with a quasi-static configuration of DL/UL subframe splitting, the detrimental DL-to-UL interference in the macrocell tier can be avoided. In contrast, the traffic behavior is completely different in the small-cell tier mostly because of the low number of connected UEs per small cell and the burstiness of their DL and UL traffic demands. This leads to drastic DL/UL traffic fluctuations, which are particularly suitable for dynamic TDD operations. Here, we propose that the macrocell tier uses a quasi-static configuration of DL/UL subframe splitting, which matches its statistical DL/UL traffic ratio, and consider dynamic TDD only for the small-cell tier.

Moreover, in a HetNet, dynamic TDD operation at small cells cannot ignore CRE and ABS operations that have already been adopted at the macrocells, and these technologies need to be designed together. Hence, the following design aspects have to be considered:

- scheduling policy in small cells, i.e., what is the behavior of small cells in macrocell DL, UL, and ABS subframes;
- UE cell association after CRE and optimal macrocell ABS duty cycle;
- dynamic TDD scheduling at small cells.

In the following, we examine these issues one by one in detail.

##### A. Scheduling Policy in Small Cells

For small-cell UEs, any UL transmission attempt to SBSs will find itself in an extremely adverse situation in the subframes aligned with macrocell DL subframes since DL signals

emitted from MBSs are of high power and, thus, can easily jam small-cell UEs' UL signals. Macrocell DL to small-cell UL IC techniques based on full or partial prior information of macrocell DL transmissions may solve this problem. However, the involved complexity in this kind of intertier IC is extremely high, considering the dominant role of the DL interference coming from macrocells and the heavy traffic flow in macrocells. Thus, it may not be wise to abuse the IC technique to cancel the DL-to-UL interference from the macrocell tier to the small-cell tier. Thus, we propose that small cells only conduct DL transmissions in the subframes aligned with macrocell DL subframes.

As for the subframes aligned with macrocell UL and ABS subframes since the interference suffered by SBSs and small-cell UEs will probably be low because strong interfering macrocell UEs are very likely to have been offloaded to small cells as ER UEs, we propose that small cells can perform dynamic TDD when macrocells transmit UL or ABS subframes.

As a result of these scheduling policies, not all subframes in the small-cell tier are dynamic TDD subframes, and the number of dynamic TDD subframes is denoted  $f^{S,dynTDD}$ .

Having decided which subframe type should be scheduled at each time at small cells, it is important to define which small-cell UEs should be scheduled in the subframes overlapping with macrocell DL subframes and in the dynamic TDD subframes. A widely adopted assumption in LTE-A DL HetNets is that DL packets of ER UEs should be scheduled with a high priority in subframes overlapping with the macrocell ABSs and that they should not be scheduled in subframes overlapping with the macrocell DL subframes due to the strong intertier interference [32]. Taking into account the previous scheduling policy and extending these ideas to the HetNet dynamic TDD scenario, we propose the following.

- 1) Small-cell DL packets of ER UEs, i.e.,  $U_n^{M2S}$ , are transmitted in small-cell dynamic TDD DL subframes.
- 2) Small-cell DL packets of non-ER UEs, i.e.,  $U_n^S$ , are transmitted in subframes overlapping with the macrocell DL subframes. If the small-cell dynamic TDD DL subframes are not occupied, DL packets of non-ER UEs can also be carried by these subframes.
- 3) Small-cell UL packets of all connected UEs, i.e.,  $U_n^S \cup U_n^{M2S}$ , are transmitted in small-cell dynamic TDD UL subframes.

##### B. UE Cell Association and Macrocell ABS Duty Cycle

In light of the CRE and ABS operations, and given the proposed scheduling policy in small cells, the next important questions to be answered are the following: To which small cell should each offloaded macrocell UE go? Which is the optimal ABS duty cycle for the macrocell tier? To answer these questions, in this paper, a new semi-dynamic algorithm is proposed to jointly determine UE cell association and macrocell ABS duty cycle, with the consideration of dynamic TDD operation at small cells.

The proposed semi-dynamic scheme considers a subframe splitting algorithm that is consistent with that presented in Section III-A, targeted at providing load balancing between the

DL and the UL average traffic demand densities, i.e., **Objective 1**. Considering the multiple cell tiers in HetNets, the proposed semi-dynamic scheme also tries to find the optimal macrocell ABS duty cycle, which achieves **Objective 3**, i.e., to minimize the average cell traffic demand density for the macrocell and the small-cell tiers, proving load balancing between tiers.

The proposed algorithm to jointly determine UE cell association and macrocell ABS duty cycle is summarized in Algorithm 2, where  $A$  is the number of ABSs given up by the macrocells every  $T$  subframes with  $A \in \{0, 1, \dots, T-1\}$ ,  $\alpha^{M,DL}$  and  $\alpha^{M,UL}$  are the ratios of DL-to-total subframes and UL-to-total subframes for macrocells, respectively, with  $\alpha^{M,DL} + \alpha^{M,UL} = 1$ , and  $\text{round}\{x\}$  is an operator that maps  $x$  to its closest integer. Moreover, and similar to the DL/UL average traffic demand densities defined in (1) and (2) for small cell  $c(n)$ , the average traffic demand densities for macrocell  $b(m)$  in the DL and the UL are, respectively, defined as

$$d_m^{M,DL} = \frac{\sum_{k=1}^{K_1(m)} \lambda_{DL}^{DL}(q_{m,k}^M)}{f^{M,DL}} \quad (9)$$

$$d_m^{M,UL} = \frac{\sum_{k=1}^{K_1(m)} \lambda_{UL}^{UL}(q_{m,k}^M)}{f^{M,UL}} \quad (10)$$

where the numerator is the sum of DATARs/UATARS  $\lambda_{DL(UL)}^{DL(UL)}(q_{m,k}^M)$  of all UEs connected to macrocell  $b(m)$ , and the denominator is the number of DL (UL) subframes in every  $T$  subframes available to transmit it, with this number being denoted  $f^{M,DL}$  ( $f^{M,UL}$ ).

---

**Algorithm 2** Joint selection of UE cell association and macrocell ABS duty cycle in a HetNet

---

**for**  $A = 0 : T - 1$  **do**

  Compute  $f^{M,DL} = \text{round}\{(T - A) \times \alpha^{M,DL}\}$ ,  $f^{M,UL} = T - A - f^{M,DL}$ , and  $f^{S,dynTDD} = f^{M,UL} + A$ .

**for**  $m = 1 : M$  **do**

    Initialization:  $U_m^M = U_m^{M*}$ ,  $K_1(m) = K_1^*(m)$ .

    Obtain  $\bar{U}_m^M$  by sorting  $u(q_{m,k}^M)$  according to the ascending order of  $\gamma_{m,k}^M$ .

**for**  $j = 1 : K_1(m)$  **do**

      Regarding the candidate ER UE  $u(q_{m,\pi(j)}^M)$ , calculate  $d_m^{M,DL}$  and  $d_m^{M,UL}$  using (11) and (12).

      Obtain  $C(q_{m,\pi(j)}^M)$  by sorting all small cells according to the descending order of  $\mu_{n,q_{m,\pi(j)}^M}^S$ .

**for**  $l = 1 : N$  **do**

      Compute  $d_{\zeta(l)}^{S,DL,M\_DL\_sf}$  using (13).

      Obtain  $t_{\zeta(l)}^{STAT\_het}$ ,  $d_{\zeta(l)}^{S,DL,dynTDD\_sf}(t_{\zeta(l)}^{STAT\_het})$  and  $d_{\zeta(l)}^{S,UL,dynTDD\_sf}(t_{\zeta(l)}^{STAT\_het})$  for the candidate outsourcing small cell  $c(\zeta(l))$  using Algorithm 3.

      Update  $d_{\zeta(l)}^{S,DL}$  and  $d_{\zeta(l)}^{S,UL}$  using (17) and (18).

**if**  $d_{\zeta(l)}^{S,DL} < d_m^{M,DL}$  **and**  $d_{\zeta(l)}^{S,UL} < d_m^{M,UL}$  **and**  $\mu_{m,q_{m,\pi(j)}^M}^M - \mu_{\zeta(l),q_{m,\pi(j)}^M}^S < y$  **then**

        UE  $u(q_{m,\pi(j)}^M)$  is outsourced to  $c(\zeta(l))$ .

        Update the UE cell association as

$K_3(\zeta(l)) = K_3(\zeta(l)) + 1$ ;

$$R_{\zeta(l)}^{M2S} = R_{\zeta(l)}^{M2S} + \{u(q_{m,\pi(j)}^M)\};$$

$$K_1(m) = K_1(m) - 1;$$

$$U_m^M = U_m^M - \{u(q_{m,\pi(j)}^M)\}.$$

      Record the average traffic demand density of macrocell  $b(m)$  as  $d_m^M(A) = (d_m^{M,DL} + d_m^{M,UL})/2$ .

      Obtain the average traffic demand density for small cell  $c(\zeta(l))$  as  $d_{\zeta(l)}^S(A) = (d_{\zeta(l)}^{S,DL} + d_{\zeta(l)}^{S,UL})/2$ .

**break**;

**end if** {judgement of a successful outsourcing}

**end for** {loop of candidate small cells}

**end for** {loop of candidate ER UEs}

**end for** {loop of macrocells}

**end for** {loop of candidate macrocell ABS duty cycles}

  Choose the appropriate macrocell ABS duty cycle using (19), and UE cell association is eventually determined based on  $A^{\text{opt}}$ .

---

It is important to note that, due to the static TDD configuration in the macrocell tier,  $f^{M,DL}$  and  $f^{M,UL}$  take networkwide values for all macrocells, and that  $f^{M,DL} + f^{M,UL} + A = T$ .

Due to the limited solution space of  $A$ , Algorithm 2 performs an exhaustive search on  $A$ , and its objective is to find the optimal  $A^{\text{opt}}$ , which achieves **Objective 3**, i.e., to minimize the average cell traffic demand density for the macrocell and small-cell tiers. Note that in practice, different operators may have different objectives and could select different optimization targets, but in those, there is always a tradeoff between the macrocell and small cell UPTs [33], i.e., increasing macrocell UPT reduces small-cell UPT and *vice versa*. Intuitively,  $A^{\text{opt}}$  tends to be larger if some operator wants to put more emphasis on the performance of the small-cell tier and *vice versa*.

The procedure of Algorithm 2 is explained as follows, where for each possible  $A$  the following operations are performed.

For each macrocell  $b(m)$ , all connected UEs in  $U_m^M$  are sorted according to their ascending order of wideband SINR  $\gamma_{m,k}^M$ , and the following sorted set is obtained  $\bar{U}_m^M = \{u(q_{m,\pi(1)}^M), \dots, u(q_{m,\pi(j)}^M), \dots, u(q_{m,\pi(K_1(m))}^M)\}$ . The first UE in the sorted set is the first candidate UE to be offloaded to a small cell, and candidate UEs are examined sequentially.

For an examined candidate UE  $u(q_{m,\pi(j)}^M)$  to be offloaded, the average DL and UL traffic demand densities for macrocell  $b(m)$  in (9) and (10) are updated as follows:

$$d_m^{M,DL} = d_m^{M,DL} - \frac{\lambda_{DL}^{DL}(q_{m,\pi(j)}^M)}{f^{M,DL}} \quad (11)$$

$$d_m^{M,UL} = d_m^{M,UL} - \frac{\lambda_{UL}^{UL}(q_{m,\pi(j)}^M)}{f^{M,UL}}. \quad (12)$$

Then, to determine the new serving cell of candidate UE  $u(q_{m,\pi(j)}^M)$ , all small cells  $c(n)$  are sorted according to their descending order of RSRP, i.e.,  $\mu_{n,q_{m,\pi(j)}^M}^S$ . The sorted small-cell set is UE specific and is denoted  $C(q_{m,\pi(j)}^M) = \{c(\zeta(1)), \dots, c(\zeta(l)), \dots, c(\zeta(N))\}$ . Because of its highest signal strength, the first small cell in the sorted set is the first candidate small cell to host the candidate UE, and candidate small cells are examined sequentially.

For each candidate small cell  $c(\zeta(l))$ , its average DL traffic demand density in the subframes overlapping with macrocell DL subframes, which is denoted by  $d_{\zeta(l)}^{S,DL,M\_DL\_sf}$  is defined as

$$d_{\zeta(l)}^{S,DL,M\_DL\_sf} = \frac{\sum_{k=1}^{K_2(\zeta(l))} \lambda^{DL} \left( q_{\zeta(l),k}^S \right)}{f^{M,DL}} \quad (13)$$

where the numerator is the sum of DATARs  $\lambda^{DL}(q_{\zeta(l),k}^S)$  of all non-ER UEs in small cell  $c(\zeta(l))$ . The proposed definition is predicated on the fact that, according to our scheduling policy, small-cell DL packets of non-ER UEs should be typically transmitted in subframes overlapping with the macrocell DL subframes, which number is  $f^{M,DL}$ .

Once the average DL traffic demand density in the subframes overlapping with macrocell DL subframes has been calculated, the algorithm looks for the statistically optimal splitting of dynamic TDD subframes in the DL and the UL for the candidate small cell  $c(\zeta(l))$ . For future use in Section IV-D, the presentation of the proposed statistically optimal splitting of dynamic TDD DL/UL subframes in the DL and the UL for a small cell is isolated from Algorithm 2 and presented in Algorithm 3. In this case, and following the same approach as in Section III-A, we propose that the statistically optimal number of dynamic TDD UL subframes for the candidate small cell  $c(\zeta(l))$  should be derived with **Objective 1**, i.e., to minimize the difference between the average DL and UL traffic demand densities. In this way, a balanced DL/UL UPT performance in such small cell can be achieved.

In Algorithm 3,  $\Upsilon^{\text{het}}$  is the set of all available TDD configurations for the considered HetNet. For a candidate number of dynamic TDD UL subframes  $t$ , based on our proposed scheduling policy, ER UE DL traffic and all UE UL traffic should be served by dynamic TDD subframes aligned with macrocell UL and ABS subframes. Considering the candidate ER UE  $u(q_{m,\pi(j)}^M)$ , the average DL and UL traffic demand density in dynamic TDD subframes for the candidate host small cell  $c(\zeta(l))$  can be respectively computed as

$$d_{\zeta(l)}^{S,DL,dynTDD\_sf}(t) = \frac{\sum_{k=1}^{K_3(\zeta(l))} \lambda^{DL} \left( r_{\zeta(l),k}^S \right) + \lambda^{DL} \left( q_{m,\pi(j)}^M \right)}{f^{S,dynTDD} - t} \quad (14)$$

$$d_{\zeta(l)}^{S,UL,dynTDD\_sf}(t) = \frac{1}{t} \left[ \sum_{k=1}^{K_2(\zeta(l))} \lambda^{UL} \left( q_{\zeta(l),k}^S \right) + \sum_{k=1}^{K_3(\zeta(l))} \lambda^{UL} \left( r_{\zeta(l),k}^S \right) + \lambda^{UL} \left( q_{m,\pi(j)}^M \right) \right] \quad (15)$$

Then, based on such computations and similar to (3) considering **Objective 1**, the statistically optimal number of dynamic TDD UL subframes for small cell  $c(\zeta(l))$  becomes

$$t_{\zeta(l)}^{\text{STAT\_het}} = \arg \min_{t=g(r), r \in \Upsilon^{\text{het}}} \left\{ \left| d_{\zeta(l)}^{S,UL,dynTDD\_sf}(t) - d_{\zeta(l)}^{S,DL,dynTDD\_sf}(t) \right| \right\} \quad (16)$$

---

**Algorithm 3** Selection of the optimal number of average dynamic TDD UL subframes, i.e.,  $t_{\zeta(l)}^{\text{STAT\_het}}$  in a HetNet

---

**for** each  $t = g(r), r \in \Upsilon^{\text{het}}$  **do**

    Compute  $d_{\zeta(l)}^{S,DL,dynTDD\_sf}(t)$  and  $d_{\zeta(l)}^{S,UL,dynTDD\_sf}(t)$  using (14) and (15), respectively.

**end for**

Select  $t_{\zeta(l)}^{\text{STAT\_het}}$  using (16).

---

Having obtained  $t_{\zeta(l)}^{\text{STAT\_het}}$ , we propose that the average DL traffic demand density for the candidate small cell  $c(\zeta(l))$ , used in the following step, should be the larger one of the average DL traffic demand density associated with ER UEs and with non-ER UEs, which is expressed as

$$d_{\zeta(l)}^{S,DL} = \max \left\{ d_{\zeta(l)}^{S,DL,dynTDD\_sf} \left( t_{\zeta(l)}^{\text{STAT\_het}} \right), d_{\zeta(l)}^{S,DL,M\_DL\_sf} \right\} \quad (17)$$

whereas the average UL traffic demand density for the candidate small cell  $c(\zeta(l))$  is

$$d_{\zeta(l)}^{S,UL} = d_{\zeta(l)}^{S,UL,dynTDD\_sf} \left( t_{\zeta(l)}^{\text{STAT\_het}} \right) \quad (18)$$

Now, before executing the offloading of candidate UE  $u(q_{m,\pi(j)}^M)$ , we propose that two constraints should be checked. First, the average traffic demand density of the candidate small cell after offloading should not be larger than that of the source macrocell to avoid small cells taking on too much of a burden and becoming new traffic bottlenecks. This is a necessary condition in the load balanced state and is mathematically formulated as  $d_{\zeta(l)}^{S,DL} < d_m^{M,DL}$  and  $d_{\zeta(l)}^{S,UL} < d_m^{M,UL}$ . Second, the link quality between the candidate ER UE and the candidate small cell should be good enough, i.e.,  $\mu_{m,q_{m,k}^M}^M - \mu_{\zeta(l),q_{m,k}^M}^S < y$ , where  $y$  is the REB parameter in decibel scale for the CRE operation. Intuitively, the proposed two constraints require that a candidate macrocell UE should be offloaded to a small cell that is neither overloaded nor far away from the concerned macrocell UE. Otherwise, the offloading will not be performed.

Once these constraints are met, the candidate UE  $u(q_{m,\pi(j)}^M)$  is offloaded to the candidate small cell  $c(\zeta(l))$ , and all related parameters are updated as described in Algorithm 2. The average traffic demand density of the offloaded macrocell  $b(m)$  is updated as  $d_m^M(A) = (d_m^{M,DL} + d_m^{M,UL})/2$ , and that of the candidate small cell  $c(\zeta(l))$  is updated as  $d_{\zeta(l)}^{S,DL}(A) = (d_{\zeta(l)}^{S,DL} + d_{\zeta(l)}^{S,UL})/2$ .

Finally, after iterating over all macrocells, all candidate UEs, and all candidate small cells, we select the macrocell ABS duty cycle  $A^{\text{opt}}$  using the following with respect to **Objective 3**, i.e., to minimize the average traffic demand density for the macrocell and the small-cell tiers:

$$A^{\text{opt}} = \arg \min_A \left\{ \frac{1}{M+N} \left[ \sum_{m=1}^M d_m^M(A) + \sum_{n=1}^N d_n^S(A) \right] \right\} \quad (19)$$

The final UE cell association is established according to the selected  $A^{\text{opt}}$ .

In the proposed Algorithm 2, two parameters need to be chosen for its operation. The first parameter is  $T$ , which can be set to 10 according to the 3GPP specifications [21] because each transmission frame consists of ten subframes in the current LTE networks. The other parameter is  $y$ , which is the REB parameter in decibels. As suggested in some previous work on CRE [32], a reasonable value of  $y$  can be  $y = 9$  dB.

### C. Discussion on the Convergence and the Complexity of Algorithm 2

Before we delve deeper into the problem of DL/UL subframe splitting in the small-cell tier, it is beneficial to have a full assessment on the convergence and the complexity of the proposed Algorithm 2, which jointly optimizes UE cell association and macrocell ABS duty cycle. Note that Algorithm 2 is a one-shot exhaustive searching algorithm with no iterative steps; thus, convergence is not an issue for Algorithm 2.

The complexity of Algorithm 2, on the other hand, could be a serious issue that may prevent its implementation in practice. In more detail, the complexity of Algorithm 2 is on the order of  $TN \sum_{m=1}^M K_1^*(m)$  because  $T$  candidate values of  $A$  and  $N$  candidate outsourcing small cells need to be tested for *each and every* macrocell UE. One way to reduce the complexity of the algorithm without compromising its performance is to adopt a macrocell-UE-specific number of candidate outsourcing small cells based on the value of  $y$ , which should be much smaller than  $N$ , because the small cells that are too far away from the considered macrocell UE do not need to go through the offloading test due to poor signal strength. Another way to reduce the complexity is to perform Algorithm 2 inside a macrocell cluster, the size of which can be adjusted based on the implementation feasibility.

Having said that, the real challenge to implement Algorithm 2 comes from the *time-variant* network, where UEs can come and go; thus, the UE cell association and the macrocell ABS duty cycle need to be updated on the fly. In more detail, it is generally feasible to execute Algorithm 2 only once for a *time-invariant* network scenario. However, when the network becomes *time variant* due to UE mobility and bursty traffic, etc., we need to frequently recall Algorithm 2, which is not practical due to its high complexity. Note that it is not necessary to consider fast time-variant networks caused by high UE mobility in the framework of HetNet dynamic TDD since UEs with high mobility will be connected to the macrocell tier only, thus avoiding handover failure issues [2]. Here, the considered time-variant network changes on the order of seconds or hundreds of milliseconds since a UE with a speed of 10 km/h will only move about 2.78 m in 1 s, and it may take seconds or tens of seconds for a UE to finish reading a webpage before requesting a new DL/UL transmission [35]. Even so, it is still infeasible to conduct the entire Algorithm 2 every time when a UE arrives at a cell or a UE leaves a cell. Therefore, we need to design new algorithms for the time-variant networks and use Algorithm 2 in the initialization stage only. Based on the best RSRP criterion of

UE association discussed in Section II, we propose to classify the events of network changing into four cases.

- Case 1: A new macrocell UE  $u(z)$  arrives at macrocell  $b(m_0)$ . Then, we have  $U_{m_0}^{M*} = U_{m_0}^{M*} \cup u(z)$  and  $K_1^*(m_0) = K_1^*(m_0) + 1$ . There are two alternatives for algorithm design.
  - Alt. 1: For macrocell  $b(m_0)$ , we perform Algorithm 2 for macrocell  $b(m_0)$  only, the complexity of which is on the order of  $TN K_1^*(m_0)$ .
  - Alt. 2: For UE  $u(z)$ , we can design a new algorithm, which is denoted by Algorithm 2-A, to check the  $N$  candidate outsourcing small cells and decide whether UE  $u(z)$  should stay in macrocell  $b(m_0)$ , or it should be offloaded to a small cell  $c(n_0)$ . The complexity of Algorithm 2-A is on the order of  $TN$ .
- Case 2: A macrocell UE  $u(q_{m_0, k_0}^M)$  leaves from macrocell  $b(m_0)$ . Then, we have  $U_{m_0}^{M*} = U_{m_0}^{M*} \setminus u(q_{m_0, k_0}^M)$  and  $K_1^*(m_0) = K_1^*(m_0) - 1$ . Moreover, there are two alternatives for algorithm design.
  - Alt. 1: For macrocell  $b(m_0)$ , we perform Algorithm 2 for macrocell  $b(m_0)$  only, the complexity of which is on the order of  $TN K_1^*(m_0)$ .
  - Alt. 2: Since a UE leaves from macrocell  $b(m_0)$ , the traffic load of macrocell  $b(m_0)$  should be reduced. Therefore, we should design a new algorithm, which is denoted by Algorithm 2-B, to examine the  $K_1^*(m_0) - K_1(m_0)$  UEs that have been outsourced to small cells and check whether some of them should come back to macrocell  $b(m_0)$ . The complexity of Algorithm 2-B is on the order of  $T[K_1^*(m_0) - K_1(m_0)]$ .
- Case 3: A new small-cell UE  $u(z)$  arrives at small cell  $c(n_0)$ . Note that such UE cannot be an ER UE because we consider the best RSRP criterion of UE association, and all the potential ER UEs should go through Case 1 first. Due to the arrival of UE  $u(z)$ , the traffic load of small cell  $c(n_0)$  should be increased. Therefore, we should design a new algorithm, which is denoted by Algorithm 2-C, to check the  $K_3(n_0)$  UEs that have been outsourced to small cell  $c(n_0)$  and check whether some of them should come back to their original macrocells. The complexity of Algorithm 2-C is on the order of  $T K_3(n_0)$ .
- Case 4: A small-cell UE  $u(q_{n_0, k_0}^S)$  leaves from small cell  $c(n_0)$ . Note that such UE can be an ER UE or a non-ER UE. Either way, the traffic load of small cell  $c(n_0)$  should be reduced. Therefore, we should design a new algorithm, which is denoted by Algorithm 2-D, to examine all the macrocell UEs, the number of which is  $\sum_{m=1}^M K_1(m)$ , and check whether some of them are eligible to be outsourced by small cell  $c(n_0)$ . The complexity of Algorithm 2-D is on the order of  $T \sum_{m=1}^M K_1(m)$ .

In this paper, we would like to focus on *time-invariant* networks, both in algorithm design and simulation, to show the full potential of dynamic TDD in HetNets. In our future work, we will study Case 1–4 and Algorithm 2-A–D for *time-variant* networks.

#### D. Dynamic DL/UL Subframe Splitting in the Small Cell Tier

Following the dynamic DL/UL subframe splitting algorithm (see Algorithm 1) proposed for the HomSCNs, we also propose a dynamic algorithm to compute the instantaneous small-cell dynamic TDD DL/UL subframe splitting for a given small cell according to its instantaneous traffic conditions in a HetNet. Similar to Algorithm 1, the proposed algorithm is performed every  $T$  subframes and is based on the criterion of **Objective 2**, i.e., to minimize the difference between the instantaneous DL and UL traffic demand densities in each small cell. Considering our previous discussion in Section IV-B, the instantaneous DL and UL traffic demand densities of  $c(n)$  for given number of dynamic UL subframes  $t$  are defined in a similar way as in (14) and (15) with  $\omega$  instead of  $\lambda$ , i.e.,

$$\begin{aligned} \tilde{d}_n^{S,DL,dynTDD\_sf}(t) &= \frac{\sum_{k=1}^{K_3(n)} \omega^{DL}(r_{n,k}^S)}{f^{S,dynTDD} - t} \quad (20) \\ \tilde{d}_n^{S,UL,dynTDD\_sf}(t) &= \frac{1}{t} \left[ \sum_{k=1}^{K_2(n)} \omega^{UL}(q_{n,k}^S) + \sum_{k=1}^{K_3(n)} \omega^{UL}(r_{n,k}^S) \right]. \quad (21) \end{aligned}$$

Then, similar to (16) considering **Objective 2**, the optimal number of instantaneous dynamic TDD UL subframes for small cell  $c(n)$  can be selected as

$$t_n^{INST\_het} = \arg \min_{t=g(r), r \in \Upsilon^{het}} \left\{ \left| \tilde{d}_n^{S,UL,dynTDD\_sf}(t) - \tilde{d}_n^{S,DL,dynTDD\_sf}(t) \right| \right\}. \quad (22)$$

---

**Algorithm 4** Selection of the optimal number of instantaneous dynamic TDD UL subframes in a small cell, i.e.,  $t_n^{INST\_het}$ , for a HetNet

---

Obtain  $f^{S,dynTDD} = f^{M,UL} + A^{opt}$  via Algorithm 2.  
 Compute  $\tilde{d}_n^{S,DL,dynTDD\_sf}(t)$  and  $\tilde{d}_n^{S,UL,dynTDD\_sf}(t)$  using (20) and (21), respectively.  
 Select  $t_n^{INST\_het}$  using the following procedure.  
**if**  $\omega^{UL}(q_{n,k}^S) = 0, \forall q_{n,k}^S \in Q_n^S$  **and**  $\omega^{UL}(r_{n,k}^S) = 0, \forall r_{n,k}^S \in R_n^{M2S}$  **and**  $\omega^{DL}(r_{n,k}^S) = 0, \forall r_{n,k}^S \in R_n^{M2S}$  **then**  
     Obtain  $t_n^{INST\_het} = t_n^{STAT\_het}$ , which is computed using Algorithm 3 with  $u(q_{m,\pi(j)}^M) = \emptyset$ .  
**else**  
     Obtain  $t_n^{INST\_het}$  using (22).  
**end if**

---

The proposed algorithm to split the dynamic TDD DL/UL subframes for small cell  $c(n)$  in a HetNet is summarized in Algorithm 4. Note that Algorithm 4 is built on the same principle as that of Algorithm 1 so that our design of dynamic TDD for small cells is coherent for both HomSCNs and HetNets. Similar to the consideration on the range of  $t$  for Algorithm 1, here, we also impose constraints on  $t$  so that the DL/UL control/reference signal channels are always available for the small-cell TDD system to function properly. Since  $f^{M,DL} \geq 1$

(the macrocell DL should never be completely deactivated), which indicates the availability of DL subframes for the small-cell tier in every  $T$  subframes, we assume that  $\Upsilon^{het}$  contains TDD configurations with  $g(r) \in [1, f^{S,dynTDD}]$ . Moreover, as indicated in Algorithm 1, when a small cell is completely idle with neither DL nor UL traffic demand, we propose that  $t_n^{INST\_het}$  should be set to  $t_n^{STAT\_het}$  so that the DL/UL subframe splitting in the small cell matches its statistical traffic pattern.

#### V. SYSTEM-LEVEL SIMULATION

To verify the effectiveness of the proposed dynamic TDD schemes, system-level simulations are used. As indicated in Section II, we concentrate our analysis on the 3GPP dynamic TDD Scenario 3 and Scenario 6, shown in Fig. 1(a) and (b), respectively. Detailed information on our system-level simulator used for this analysis can be found in [34]. The full list of system parameters and traffic modeling methodology can be found in [26] and [35], respectively. Some key parameters in our simulations are presented in Table II.

In our simulations, the traffic model is assumed Poisson distributed with  $\lambda^{DL}(u(q))$  taking a uniform value for all UEs [26]. Different values of  $\lambda^{DL}(u(q))$  correspond to different traffic load conditions, i.e., low, medium, and high traffic loads. Moreover,  $\lambda^{UL}(u(q))$  is assumed to be half of  $\lambda^{DL}(u(q))$ , i.e.,  $\lambda^{UL}(u(q)) = (1/2)\lambda^{DL}(u(q))$  [26]. The packet size is 0.5 MB. Packets are independently generated for the DL and the UL in each small cell, and they are randomly assigned to small-cell UEs. Finally, we assume that  $T = 10$  [21].

Due to the inherently different topology of HomSCNs and HetNets and the CRE and eCIC operations in HetNets, it is generally very difficult to accurately compare the performance of two networks, respectively, associated with Scenarios 3 and 6. Nevertheless, in the following, we will try to draw some useful conclusions regarding the comparison of dynamic TDD in HomSCNs and that in HetNets. To that end, in our simulations, as suggested in [26], we deploy ten UEs per small cell in Scenario 3, whereas we deploy ten UEs per macrocell and five UEs per small cell in Scenario 6. Therefore, the simulated Scenario 3 network is slightly more crowded with UEs than the simulated Scenario 6 network. As a result, for Scenario 3, the values of  $\lambda^{DL}(u(q))$  are set to {0.05, 0.25, 0.45} packets per UE per second to represent the low, medium, and high traffic loads, respectively. In contrast, for Scenario 6 to achieve a similar load, the values of  $\lambda^{DL}(u(q))$  are slightly increased to {0.1, 0.3, 0.5} packets per UE per second due to its relatively lower UE density. Note that, here, we assume  $\lambda^{DL}(u(q))$  is independent of the UE index  $q$  because we want to focus on a case with the same  $\lambda^{DL}(u(q))$  for all UEs. This facilitates the extraction of conclusions on the functioning of dynamic TDD and interference mitigation techniques that are not biased by the traffic model. However, it should be clarified that no restriction is imposed on the values of  $\lambda^{DL}(u(q))$  in the proposed algorithms, which ensures their feasibility in general cases. Moreover, note that the aggregate traffic load for each cell should be the product of  $\lambda^{DL}(u(q))$  and the number of served UEs, which roughly injects more than four packets

TABLE II  
KEY SIMULATION PARAMETERS

Parameters	Assumptions
Scenario	Scenario 3 or Scenario 6 [26]
Network layout	7 cell sites, 3 macrocells per cell site, wrap-around
Inter-site distance	500 m [35]
# small cells per macrocell	4 (84 small cells in total) [26]
Small cell deployment	Random deployment, 40 m radius of coverage [26]
# UEs per macrocell	0 (Scenario 3), 10 (Scenario 6) [26]
# UEs per small cell	10 (Scenario 3), 5 (Scenario 6) [26]
System bandwidth	10 MHz [35]
UE deployment	Uniform and random deployment in cell coverage
# macro/small cell antenna	4 (for both transmission and reception)
# UE antenna	2 (for both transmission and reception)
Receiver type	Basic MMSE Rx for both the DL and the UL [26]
Codebook for PMI feedback	LTE Release 11 codebook with WB rank adaptation
UE scheduling in each cell	Proportional fairness (PF)
Packet scheduling for each UE	Round Robin (RR)
Modulation & coding schemes	QPSK, 16QAM, 64QAM, 256 QAM
Ideal genie-aided LA	Target BLER being 0.1 for both the DL and the UL
IC capability	For DL: none For UL: with or without perfect DL-to-UL IC
Non-data overhead	3 out of 14 OFDM symbols per subframe
HARQ modelling	Retransmission in the first available subframe
Small-scale fading channel	Explicitly modelled (EPA channel [36])

into each small per second in case of high traffic load, i.e.,  $\lambda^{\text{DL}}(u(q)) = 0.45$ .

With regard to key performance indicators, UPT is adopted in this paper. According to [35], UPT is defined as the ratio of successfully transmitted bits over the time consumed to transmit the said data bits, where the consumed time starts when the DL/UL packet arrives at the UE DL/UL buffer and ends when the last bit of the DL/UL packet is correctly decoded.

It is important to note that an ideal genie-aided LA mechanism is adopted for both HomSCNs and HetNets in this paper. In more detail, appropriate modulation and coding schemes are chosen according to the perceived SINRs *after* the DL/UL transmissions. We make such assumption due to the following reasons.

- Some results in our previous work on dynamic TDD [24], [27] were lacking insight and seemed counterintuitively small because a simple LA mechanism was assumed therein; hence, the true value of dynamic TDD was not fully revealed as a result of using such a nonideal practical link adapter.
- To make a fair performance comparison between dynamic TDD in HomSCNs and in HetNets, a common LA algorithm should be assumed, and the ideal genie-aided LA mechanism is a good choice since it provides the performance upper bounds for the considered networks.
- As can be well imagined, the fluctuation of interference in dynamic TDD transmissions should be significantly larger than that in static TDD ones. How to harness such interference fluctuation and perform a good LA function in practical networks are far from trivial and are out of the scope of this paper. Therefore, considering an ideal genie-aided LA mechanism becomes the logical choice.

It is also important to note that, in both our algorithm design and our simulation evaluation, we adopt some ideal assumptions such as the ideal genie-aided LA mechanism, the perfect

intercell IC function (if considered), the perfect knowledge of  $\omega^{\text{DL}}(q)$  and  $\omega^{\text{UL}}(q)$  for the instantaneous splitting of dynamic TDD subframes, etc. Our intention is to conduct a performance evaluation to show the *potentials* of dynamic TDD in current and future networks, and it will be our future work to consider more practical assumptions in this paper. For example, although it is feasible for a UE to report its UL buffer size to its serving BS in the LTE networks, some mismatch between the reported buffer size and the actual one still exists due to the quantization error and the feedback error [2]. Such errors should be considered properly in a more detailed study.

## VI. HOMOGENEOUS SMALL-CELL NETWORK RESULTS

Here, we present numerical results to compare the performance of the existing static TDD scheme in LTE Release 11 with that of dynamic TDD transmissions in LTE Release 12 and an enhanced version with full flexibility of dynamic TDD configuration, which probably falls into the scope of LTE future releases. We also investigate the performance gains of dynamic TDD with the basic ILIM schemes presented in Section III-B and their combinations. The study is performed for  $\lambda^{\text{DL}}(u(q)) = \{0.05, 0.25, 0.45\}$ , as explained in Section V.

For LTE future releases, apart from the existing seven TDD configurations defined for  $\Upsilon^{\text{homo}}$  in LTE Release 12, another three TDD configurations favoring the UL transmissions with DL/UL subframe ratios of 1/9, 2/8, and 3/7, respectively, are added to  $\Upsilon^{\text{homo}}$ . It should be noted that the DL/UL subframe ratio in LTE Release 12 cannot go below 2/3 [21], whereas in the hypothetical LTE future release network, the ratio now ranges freely from 1/9 to 9/1; hence, the system can achieve full flexibility of dynamic TDD configuration. The purpose of investigating a hypothetical  $\Upsilon^{\text{homo}}$  of LTE future releases is to check the performance limit.

Considering the ILIM schemes addressed in Section III-B, the corresponding parameters are explained in the following.

TABLE III  
RELATIVE PERFORMANCE GAINS OF DL AND UL UPTS (HOMSCN, BASIC ILIM)

95-percentile UPTs	Sch. 1 (Mbps)	Sch. 2	Sch. 3	Sch. 4	Sch. 5	Sch. 6	Sch. 6(a)	Sch. 6(b)	Sch. 7
DL $\lambda^{\text{DL}}(u(q)) = 0.05$	62.50 (-)	4.92%	25.49%	25.49%	25.49%	25.49%	25.49%	25.49%	25.49%
DL $\lambda^{\text{DL}}(u(q)) = 0.25$	57.97 (-)	1.47%	25.45%	23.21%	27.78%	25.45%	25.45%	25.45%	27.78%
DL $\lambda^{\text{DL}}(u(q)) = 0.45$	47.06 (-)	-4.49%	23.19%	11.70%	34.92%	28.40%	23.19%	25.00%	32.81%
UL $\lambda^{\text{UL}}(u(q)) = 0.05/2$	13.75 (-)	78.53%	100.69%	102.08%	246.43%	106.38%	102.08%	103.50%	212.90%
UL $\lambda^{\text{UL}}(u(q)) = 0.25/2$	12.66 (-)	70.81%	88.10%	89.22%	232.63%	106.54%	97.50%	100.00%	219.19%
UL $\lambda^{\text{UL}}(u(q)) = 0.45/2$	10.84 (-)	57.69%	80.88%	74.06%	229.46%	108.42%	88.27%	93.19%	229.46%
50-percentile UPTs	Sch. 1 (Mbps)	Sch. 2	Sch. 3	Sch. 4	Sch. 5	Sch. 6	Sch. 6(a)	Sch. 6(b)	Sch. 7
DL $\lambda^{\text{DL}}(u(q)) = 0.05$	38.83 (-)	-7.21%	24.10%	19.77%	27.16%	24.10%	23.03%	22.62%	24.10%
DL $\lambda^{\text{DL}}(u(q)) = 0.25$	23.12 (-)	-4.42%	16.11%	-0.29%	30.08%	22.26%	20.56%	20.98%	21.00%
DL $\lambda^{\text{DL}}(u(q)) = 0.45$	7.18 (-)	14.61%	21.24%	-1.07%	52.39%	48.14%	28.34%	41.01%	53.02%
UL $\lambda^{\text{UL}}(u(q)) = 0.05/2$	11.46 (-)	63.85%	92.82%	92.82%	245.54%	98.86%	96.07%	94.97%	195.76%
UL $\lambda^{\text{UL}}(u(q)) = 0.25/2$	6.98 (-)	74.43%	91.64%	94.90%	239.05%	143.83%	119.54%	131.98%	258.13%
UL $\lambda^{\text{UL}}(u(q)) = 0.45/2$	3.18 (-)	61.70%	69.77%	77.68%	191.88%	156.73%	95.65%	135.36%	209.09%
5-percentile UPTs	Sch. 1 (Mbps)	Sch. 2	Sch. 3	Sch. 4	Sch. 5	Sch. 6	Sch. 6(a)	Sch. 6(b)	Sch. 7
DL $\lambda^{\text{DL}}(u(q)) = 0.05$	17.32 (-)	1.03%	21.80%	13.99%	26.92%	22.87%	20.06%	19.93%	20.27%
DL $\lambda^{\text{DL}}(u(q)) = 0.25$	2.76 (-)	65.84%	65.83%	21.91%	91.71%	113.02%	113.64%	98.14%	114.52%
DL $\lambda^{\text{DL}}(u(q)) = 0.45$	0.50 (-)	35.11%	26.84%	6.16%	69.19%	90.02%	70.66%	90.03%	99.06%
UL $\lambda^{\text{UL}}(u(q)) = 0.05/2$	6.26 (-)	90.03%	125.42%	116.44%	275.59%	133.67%	129.68%	124.82%	224.94%
UL $\lambda^{\text{UL}}(u(q)) = 0.25/2$	2.31 (-)	84.91%	120.20%	141.03%	225.14%	212.25%	181.79%	202.44%	285.11%
UL $\lambda^{\text{UL}}(u(q)) = 0.45/2$	0.71 (-)	6.19%	3.60%	42.26%	48.28%	114.41%	65.98%	103.73%	125.52%

For the CC scheme, the coupling loss threshold  $\text{PL}^{\text{CC}}$  for small cells within a cell cluster is chosen as 90 dB [26]. For the ULPB scheme,  $\Delta P^{\text{UL}}$  is set to 10 dB [29]. For the UOIC scheme, the parameter  $x_1$  is set to  $x_1 = 9$  dB so that about half of the UEs are labeled as cell-edge UEs and treated in IC in our simulations, reducing the complexity by approximately 50% compared with the full IC scheme. Moreover, for the BOIC scheme, the parameter  $x_2$  is chosen as  $x_2 = 120$  dB, leading to around 2.3 BSs treated in IC on average in our simulations. As a result, the complexity of the BOIC scheme is slashed to approximately  $2.3/83 \approx 2.77\%$  compared with the full IC scheme (83 neighboring BSs in our simulations). Note that an additional parametric study for the proposed UOIC and BOIC schemes could be useful. However, the basic conclusion should be obvious: Different  $x_1$  and  $x_2$  parameters can achieve difference balances between complexity and performance, i.e., the proposed UOIC (BOIC) scheme will become the full IC scheme with the highest complexity when  $x_1(x_2)$  approaches infinity, and the proposed UOIC (BOIC) scheme will degenerate to the non-IC scheme with the lowest complexity when  $x_1(x_2)$  approaches zero. To keep our discussion concise and concentrate on the complexity reduction of the proposed partial IC schemes, we omit the parametric study and directly show the efficiency of the proposed UOIC/BOIC scheme using the parameters that achieve comparable performance with the full IC scheme.

#### A. Performance of DL/UL UPTs With Basic ILIM

Here, we investigate the performance of DL/UL UPTs for dynamic TDD with various basic ILIM schemes.

- Scheme 1: LTE Release 12 baseline static TDD with TDD configuration 3 as in [21], where the DL/UL subframe

ratio is 7:3. Note that the assumed TDD DL/UL subframe splitting optimally matches the ratio of  $\lambda^{\text{DL}}(u(q))$  over  $\lambda^{\text{UL}}(u(q))$  when  $T = 10$ ;

- Scheme 2: LTE Release 12 dynamic TDD ( $T_0$ ) with no ILIM;
- Scheme 3: LTE Release 12 dynamic TDD ( $T_1$ ) with no ILIM;
- Scheme 4: Scheme 3 with CC;
- Scheme 5: Scheme 3 with ULPB;
- Scheme 6: Scheme 3 with full IC;
- Scheme 6(a): Scheme 3 with UOIC;
- Scheme 6(b): Scheme 3 with BOIC;
- Scheme 7: Hypothetical LTE future release dynamic TDD ( $T_1$ ) with full IC.

Here, the periodicities of dynamic TDD reconfiguration are  $T_0 = 200$  ms and  $T_1 = 10$  ms for comparison purposes. Schemes 6(a) and 6(b) are the proposed partial IC schemes previously discussed in Section III-B.

Table III shows the relative performance gains of dynamic TDD with basic ILIM compared with the static TDD scheme (Scheme 1) in terms of 95-, 50-, and five-percentile DL/UL UPTs, respectively. The absolute results for Scheme 1 are also provided in Table III so that the absolute results for other schemes can be easily derived.

Compared with the baseline static TDD scheme (Scheme 1), the straightforward dynamic TDD scheme with  $T_1$  (Scheme 3) shows solid gains in most performance categories. However, it shows no gain in terms of the five-percentile UL UPT when the traffic load is high, i.e.,  $\lambda^{\text{DL}}(u(q)) = 0.45$ . This is due to the lack of ILIM to mitigate the DL-to-UL interference. Moreover, a faster dynamic TDD configuration timescale (Scheme 3) is shown to outperform a slower one (Scheme 2) in almost every performance category, as previously reported in [23] and [24].

To improve performance in terms of the five-percentile UL UPT, the CC scheme (Scheme 4) can be adopted. Note that the efficiency of the CC scheme degrades when the traffic grows since the flexibility of dynamic TDD is reduced as all the small cells in a cluster adapt their TDD configuration according to the aggregated traffic in the cluster rather than to their individual traffic conditions. Still, CC brings a considerable improvement of 42.26% in the five-percentile UL UPT when the traffic load is high, i.e.,  $\lambda^{\text{DL}}(u(q)) = 0.45$  at the expense of 10%–20% sacrifice in DL UPTs compared with the straightforward dynamic TDD scheme (Scheme 3).

The ULPB scheme (Scheme 5) is also quite useful to boost the UL UPTs by 225.14%–275.59% when the traffic load is low to medium, i.e.,  $\lambda^{\text{DL}}(u(q)) \leq 0.25$ , indicating that the UL network is generally power limited. However, when the traffic load is high, i.e.,  $\lambda^{\text{DL}}(u(q)) = 0.45$ , the performance gain in terms of the five-percentile UL UPT, albeit considerable, decreases by 48.28%, since the power headroom of a cell-edge UE tends to be quickly drained up and increasing UL power leads to more serious UL interference. Overall, ULPB follows a similar trend as CC.

The IC schemes (Schemes 6 and 7) are shown to bring substantial gains in every performance category compared with the baseline static TDD scheme (Schemes 1), for all the considered traffic loads. In particular, among the considered ILIM schemes, the IC schemes (Schemes 6 and 7) provide the largest performance gain of 114.41%–125.52% in terms of the five-percentile UL UPT with no loss in the DL UPTs when the traffic load is relatively high, e.g.,  $\lambda^{\text{DL}}(u(q)) = 0.45$ .

As for the proposed partial IC schemes, it is interesting to find that the BOIC scheme [see Scheme 6(b)] achieves similar results with small losses in every performance category compared with the full IC scheme (see Scheme 6). This is because, in current networks where small cells are not ultradensely deployed, only a few BSs are the dominant interferers. Thus, canceling the DL-to-UL interference from those BSs is already good enough to achieve satisfactory performances [21]. In contrast, the UOIC scheme [see Scheme 6(a)] turns out to be much less effective than the BOIC scheme [see Schemes 6(b)], particularly in improving UL UPTs when the traffic load is medium to high. This is because in realistic scenarios cell-center UEs are also vulnerable to dominant DL-to-UL interference in dynamic TDD since BS-to-BS path loss could be orders of magnitude smaller than UE-to-BS path loss [21]. As a result, even a cell-center UE with good link quality cannot combat such a large difference in signal reception levels. Thus, we conclude that, if partial IC should be used to reduce the complexity/cost of full IC, the BOIC scheme is a much more preferable choice than the UOIC scheme.

Another important note is that compared with our previous work on dynamic TDD in HomSCNs [24], the performance gains of dynamic TDD are considerably larger in this paper. In particular, unlike that in [24], the straightforward dynamic TDD scheme (Scheme 3) is shown to be able to work on its own with positive gains in all performance categories over the baseline Scheme 1. This is because an ideal genie-aided LA mechanism is used, as discussed in Section V so that the full potential of dynamic TDD in HomSCNs can be exposed. This shows the

importance of LA and the need for designing a practical LA algorithm in dynamic TDD networks, which will be part of our future work.

As a summary, dynamic TDD provides substantial UPT gains compared with the static TDD, the gains depending on the quality of the considered ILIM scheme. The (partial) IC schemes have been shown to provide the most significant gains at the expense of a higher complexity, and such performance gain in terms of the five-percentile UL UPT becomes much more obvious when the traffic load is medium to heavy, where the DL-to-UL interference occurs frequently.

### B. Performance of DL/UL UPTs With Combined ILIM

In the following, the following combined ILIM schemes are considered:

- Scheme 8: Combined Schemes 4 and 5;
- Scheme 9: Combined Schemes 4 and 6;
- Scheme 10: Combined Schemes 5 and 6;
- Scheme 10(b): Combined Schemes 5 and 6(b);
- Scheme 11: Combined Schemes 4, 5, and 6;
- Scheme 12: Combined Schemes 5 and 7.

Table IV shows the relative performance gains of dynamic TDD with combined ILIM compared with the static TDD scheme (Scheme 1) in terms of 95-, 50-, and five-percentile DL/UL UPTs. Note that the absolute results for Scheme 1 are also provided in Table IV so that the absolute results for other schemes can be easily obtained.

As can be observed in Table IV, the combined CC and ULPB scheme (Scheme 8) is strictly superior to the combined CC and IC scheme (Scheme 9). This is because the CC scheme and IC scheme are somehow redundant, i.e., the CC scheme already eliminates dominant interfering small cells for the UL by coordination, rendering the IC process less effective. When the traffic load is relatively heavy, e.g.,  $\lambda^{\text{DL}}(u(q)) = 0.45$ , Scheme 8 greatly outperforms the static TDD scheme (Scheme 1) by 25.00%–62.68% and 162.55%–250.42% in terms of the DL and the UL UPTs, respectively.

The combined ULPB and IC scheme (Schemes 10) is the most powerful combination, which substantially increases the UL performance due to the larger transmit power at UEs and the IC capabilities at BSs. Some of the tremendous performance gains in the UL is also shown to be transferred to the DL by means of the traffic-adaptive dynamic TDD scheduling. To be more specific, since the performance in the UL is enhanced, some UL subframes can be transformed into DL subframes, thus improving the DL performance. When the traffic load is medium to high, e.g.,  $\lambda^{\text{DL}}(u(q)) \geq 0.25$ , Scheme 10 is shown to significantly outperform the static TDD scheme (Scheme 1) by 27.78%–153.39% and 263.22–539.48% in terms of the DL and the UL UPTs, respectively. To reduce the complexity of IC, the combination of the ULPB and the BOIC schemes (Scheme 10(b)) is proposed here. As can be seen from Table IV, Schemes 10(b) achieves a similar UPT performance compared with Schemes 10, but with a much lower complexity of the IC operations.

TABLE IV  
RELATIVE PERFORMANCE GAINS OF DL AND UL UPTs (HOMSCN, COMBINED ILIM)

95-percentile UPTs	Sch. 1 (Mbps)	Sch. 8	Sch. 9	Sch. 10	Sch. 10(b)	Sch. 11	Sch. 12
DL $\lambda^{\text{DL}}(u(q)) = 0.05$	62.50 (-)	25.49%	25.49%	25.49%	25.49%	25.49%	25.49%
DL $\lambda^{\text{DL}}(u(q)) = 0.25$	57.97 (-)	25.45%	23.21%	27.78%	27.78%	25.45%	27.78%
DL $\lambda^{\text{DL}}(u(q)) = 0.45$	47.06 (-)	25.00%	13.33%	34.92%	34.92%	25.00%	37.10%
UL $\lambda^{\text{UL}}(u(q)) = 0.05/2$	13.75 (-)	246.43%	104.93%	250.60%	246.43%	250.60%	429.09%
UL $\lambda^{\text{UL}}(u(q)) = 0.25/2$	12.66 (-)	243.48%	100.00%	263.22%	255.06%	255.06%	454.39%
UL $\lambda^{\text{UL}}(u(q)) = 0.45/2$	10.84 (-)	241.67%	91.19%	288.42%	272.73%	258.25%	495.16%
50-percentile UPTs	Sch. 1 (Mbps)	Sch. 8	Sch. 9	Sch. 10	Sch. 10(b)	Sch. 11	Sch. 12
DL $\lambda^{\text{DL}}(u(q)) = 0.05$	38.83 (-)	24.10%	19.77%	27.16%	24.10%	22.62%	28.75%
DL $\lambda^{\text{DL}}(u(q)) = 0.25$	23.12 (-)	20.14%	1.17%	36.45%	36.22%	18.49%	35.69%
DL $\lambda^{\text{DL}}(u(q)) = 0.45$	7.18 (-)	40.83%	4.14%	85.67%	83.83%	45.81%	84.44%
UL $\lambda^{\text{UL}}(u(q)) = 0.05/2$	11.46 (-)	252.53%	96.07%	259.79%	252.53%	254.01%	428.79%
UL $\lambda^{\text{UL}}(u(q)) = 0.25/2$	6.98 (-)	276.97%	104.64%	381.51%	369.67%	292.47%	653.95%
UL $\lambda^{\text{UL}}(u(q)) = 0.45/2$	3.18 (-)	250.42%	92.94%	437.61%	419.71%	267.84%	580.00%
5-percentile UPTs	Sch. 1 (Mbps)	Sch. 8	Sch. 9	Sch. 10	Sch. 10(b)	Sch. 11	Sch. 12
DL $\lambda^{\text{DL}}(u(q)) = 0.05$	17.32 (-)	23.53%	16.29%	29.05%	25.34%	23.76%	26.07%
DL $\lambda^{\text{DL}}(u(q)) = 0.25$	2.76 (-)	79.97%	52.70%	136.06%	126.26%	59.93%	151.90%
DL $\lambda^{\text{DL}}(u(q)) = 0.45$	0.50 (-)	62.68%	17.99%	153.39%	137.10%	56.98%	171.25%
UL $\lambda^{\text{UL}}(u(q)) = 0.05/2$	6.26 (-)	291.72%	117.18%	331.42%	317.32%	291.72%	480.45%
UL $\lambda^{\text{UL}}(u(q)) = 0.25/2$	2.31 (-)	353.66%	162.18%	539.48%	518.94%	369.65%	597.27%
UL $\lambda^{\text{UL}}(u(q)) = 0.45/2$	0.71 (-)	162.55%	53.74%	303.12%	287.03%	183.24%	366.93%

Finally, the combination of all three ILIM schemes (Scheme 11) only gives similar performance as that of the combination of CC and ULPB (Scheme 8), which does not justify the employment of IC on top of the joint operation of CC and ULPB. This is again because the CC scheme and IC scheme are somehow redundant. Moreover, the combined ULPB and IC scheme with full flexibility of dynamic TDD configuration (Schemes 12) is investigated to show the performance upper bound. As shown Table IV, Scheme 12 significantly outperforms the static TDD scheme (Scheme 1) by 25.49%–171.25% and 366.93%–653.95% in terms of the DL and the UL UPTs, respectively.

To sum up, if it is preferable to find an easy-to-implement scheme with reasonable performance gains, Scheme 8 should be called upon. However, if complexity issue is a minor concern, Scheme 10(b) should be engaged to realize the full potential of dynamic TDD.

## VII. HETEROGENEOUS NETWORKS RESULTS

Here, we present numerical results to benchmark the performance of static/dynamic TDD in HetNets.

We assume that the REB is  $y = 9$  dB, as suggested in some previous work on CRE [32]. Moreover, this paper is performed for  $\lambda^{\text{DL}}(u(q)) = \{0.1, 0.3, 0.5\}$ , as explained in Section V. For the considered HetNet, after running Algorithm 2, we found that  $f^{M,\text{DL}} = 5$ ,  $f^{M,\text{UL}} = 3$ ,  $A^{\text{opt}} = 2$ , and that approximately 1/3 of macrocell UEs are offloaded to small cells. Thus, five subframes in every ten subframes are used as dynamic TDD subframes in small cells, i.e.,  $f^{S,\text{dynTDD}} = 5$ .

In this light, the following schemes are considered for benchmarking.

- Scheme A (Static TDD scheme without CRE and ABS): LTE Release 12 TDD configuration 3 for both macrocells and small cells (DL/UL subframe ratio = 7:3 [21]);

- Scheme B (Straightforward dynamic TDD scheme without CRE and ABS): macrocell (DL/UL subframe ratio = 7:3), small cell (dynamic TDD without CRE and ABS). Note that Algorithm 2 is used to determine the dynamic TDD DL/UL subframe splitting for the small cells;
- Scheme C (Static TDD scheme with CRE and ABS): macrocell (DL/ABS/UL subframe ratio = 5:2:3), small cell (DL/UL subframe ratio = 7:3). Note that the scheduling policy in [32] is adopted where DL packets of ER UEs should be scheduled with a high priority in subframes overlapping with the macrocell ABSs and that they should not be scheduled in subframes overlapping with the macrocell DL subframes;
- Scheme D (Proposed scheme without IC): macrocell (DL/ABS/UL subframe ratio = 5:2:3), small cell (DL/dynamic TDD subframe ratio = 5:5), dynamic TDD reconfiguration per 10 ms, and no IC;
- Scheme E: Scheme D plus small-cell DL to macrocell UL IC;
- Scheme F: Scheme E plus small-cell DL to small-cell UL full IC, i.e., Scheme 6 in Section VI;
- Scheme F(b): Scheme E plus the BS oriented small-cell DL to small-cell UL partial IC, i.e., Scheme 6(b) in Section VI.

Table V shows the relative performance gains of the considered schemes compared with the baseline static TDD scheme (Scheme A) in terms of 95-, 50-, and five-percentile DL/UL UPTs. Note that the absolute results for Scheme A are also provided in Table V so that the absolute results for other schemes can be easily obtained. Moreover, in Table V, apart from the overall performances, the UPT results are broken down to show the contributions from the macrocell and the small-cell tiers, respectively.

TABLE V  
RELATIVE PERFORMANCE GAINS OF DL AND UL UPTs (HETNETS)

95-percentile UPTs (overall)	Sch. A (Mbps)	Sch. B	Sch. C	Sch. D	Sch. E	Sch. F	Sch. F(b)
DL $\lambda^{DL}(u(q)) = 0.1$	42.55 (-)	11.90%	9.30%	38.24%	40.30%	38.24%	38.24%
DL $\lambda^{DL}(u(q)) = 0.3$	15.81 (-)	54.75%	91.88%	155.56%	155.56%	158.16%	158.16%
DL $\lambda^{DL}(u(q)) = 0.5$	11.20 (-)	63.76%	97.40%	166.42%	162.50%	166.42%	164.44%
UL $\lambda^{UL}(u(q)) = 0.1/2$	13.58 (-)	-25.99%	17.81%	79.59%	79.92%	83.28%	82.94%
UL $\lambda^{UL}(u(q)) = 0.3/2$	12.16 (-)	-30.00%	14.46%	71.35%	72.25%	95.83%	84.83%
UL $\lambda^{UL}(u(q)) = 0.5/2$	11.50 (-)	-32.21%	10.05%	50.54%	47.63%	75.63%	65.28%
50-percentile UPTs (overall)	Sch. A (Mbps)	Sch. B	Sch. C	Sch. D	Sch. E	Sch. F	Sch. F(b)
DL $\lambda^{DL}(u(q)) = 0.1$	17.62 (-)	21.39%	18.23%	36.75%	36.75%	36.75%	36.75%
DL $\lambda^{DL}(u(q)) = 0.3$	2.19 (-)	41.86%	285.02%	432.07%	425.94%	435.19%	422.92%
DL $\lambda^{DL}(u(q)) = 0.5$	0.88 (-)	27.83%	299.10%	476.37%	468.79%	488.31%	478.20%
UL $\lambda^{UL}(u(q)) = 0.1/2$	9.96 (-)	-36.77%	7.07%	45.47%	56.84%	59.33%	57.05%
UL $\lambda^{UL}(u(q)) = 0.3/2$	3.20 (-)	-84.26%	121.28%	176.60%	188.07%	215.71%	201.26%
UL $\lambda^{UL}(u(q)) = 0.5/2$	1.29 (-)	-80.67%	267.63%	317.01%	326.45%	399.47%	368.58%
5-percentile UPTs (overall)	Sch. A (Mbps)	Sch. B	Sch. C	Sch. D	Sch. E	Sch. F	Sch. F(b)
DL $\lambda^{DL}(u(q)) = 0.1$	6.13 (-)	7.95%	4.34%	37.84%	37.84%	38.72%	38.72%
DL $\lambda^{DL}(u(q)) = 0.3$	0.16 (-)	21.51%	439.40%	492.22%	493.72%	494.22%	493.72%
DL $\lambda^{DL}(u(q)) = 0.5$	0.09 (-)	3.71%	153.15%	172.46%	170.47%	171.55%	170.28%
UL $\lambda^{UL}(u(q)) = 0.1/2$	3.43 (-)	-61.65%	51.94%	-25.50%	78.90%	79.34%	79.34%
UL $\lambda^{UL}(u(q)) = 0.3/2$	0.30 (-)	-84.21%	380.98%	-74.29%	413.76%	417.71%	412.59%
UL $\lambda^{UL}(u(q)) = 0.5/2$	0.13 (-)	-72.09%	165.06%	-57.66%	193.40%	210.47%	205.88%
95-percentile UPTs (macrocells)	Sch. A (Mbps)	Sch. B	Sch. C	Sch. D	Sch. E	Sch. F	Sch. F(b)
DL $\lambda^{DL}(u(q)) = 0.1$	47.20 (-)	0.47%	-10.79%	-10.79%	-11.58%	-10.79%	-10.79%
DL $\lambda^{DL}(u(q)) = 0.3$	6.04 (-)	18.61%	209.90%	215.82%	215.82%	215.97%	212.83%
DL $\lambda^{DL}(u(q)) = 0.5$	2.92 (-)	9.59%	159.20%	174.26%	170.47%	174.26%	174.26%
UL $\lambda^{UL}(u(q)) = 0.1/2$	13.08 (-)	-33.71%	24.69%	-20.20%	26.38%	29.00%	27.33%
UL $\lambda^{UL}(u(q)) = 0.3/2$	5.12 (-)	-87.22%	70.14%	-76.66%	89.80%	89.80%	89.71%
UL $\lambda^{UL}(u(q)) = 0.5/2$	2.08 (-)	-86.27%	152.76%	-79.34%	184.90%	185.24%	177.72%
50-percentile UPTs (macrocells)	Sch. A (Mbps)	Sch. B	Sch. C	Sch. D	Sch. E	Sch. F	Sch. F(b)
DL $\lambda^{DL}(u(q)) = 0.1$	17.47 (-)	0.00%	8.53%	9.05%	9.05%	9.57%	9.31%
DL $\lambda^{DL}(u(q)) = 0.3$	0.89 (-)	4.73%	295.75%	308.74%	309.48%	309.11%	306.51%
DL $\lambda^{DL}(u(q)) = 0.5$	0.29 (-)	5.66%	265.23%	282.56%	282.06%	285.02%	283.83%
UL $\lambda^{UL}(u(q)) = 0.1/2$	8.02 (-)	-51.97%	23.51%	-36.07%	26.01%	26.33%	25.69%
UL $\lambda^{UL}(u(q)) = 0.3/2$	1.03 (-)	-88.27%	247.12%	-79.87%	272.84%	280.16%	275.01%
UL $\lambda^{UL}(u(q)) = 0.5/2$	0.44 (-)	-80.54%	171.67%	-73.01%	209.91%	220.84%	214.40%
5-percentile UPTs (macrocells)	Sch. A (Mbps)	Sch. B	Sch. C	Sch. D	Sch. E	Sch. F	Sch. F(b)
DL $\lambda^{DL}(u(q)) = 0.1$	5.72 (-)	-4.45%	13.88%	20.41%	20.24%	21.01%	21.07%
DL $\lambda^{DL}(u(q)) = 0.3$	0.12 (-)	14.05%	298.88%	305.64%	307.90%	309.19%	308.71%
DL $\lambda^{DL}(u(q)) = 0.5$	0.08 (-)	0.31%	91.85%	95.06%	94.94%	96.29%	95.36%
UL $\lambda^{UL}(u(q)) = 0.1/2$	2.87 (-)	-65.84%	53.68%	-41.92%	62.30%	62.99%	61.79%
UL $\lambda^{UL}(u(q)) = 0.3/2$	0.23 (-)	-82.38%	249.81%	-76.62%	268.03%	274.18%	268.29%
UL $\lambda^{UL}(u(q)) = 0.5/2$	0.11 (-)	-74.12%	58.54%	-68.27%	73.05%	82.26%	76.25%
95-percentile UPTs (small cells)	Sch. A (Mbps)	Sch. B	Sch. C	Sch. D	Sch. E	Sch. F	Sch. F(b)
DL $\lambda^{DL}(u(q)) = 0.1$	36.94 (-)	29.39%	38.84%	74.67%	74.67%	74.67%	74.67%
DL $\lambda^{DL}(u(q)) = 0.3$	20.00 (-)	53.61%	66.67%	122.22%	117.39%	122.22%	117.39%
DL $\lambda^{DL}(u(q)) = 0.5$	15.29 (-)	51.56%	61.63%	112.68%	111.22%	115.14%	114.50%
UL $\lambda^{UL}(u(q)) = 0.1/2$	13.85 (-)	-23.40%	13.81%	80.56%	80.56%	85.19%	82.85%
UL $\lambda^{UL}(u(q)) = 0.3/2$	12.83 (-)	-31.52%	15.87%	70.37%	68.57%	91.22%	86.70%
UL $\lambda^{UL}(u(q)) = 0.5/2$	12.38 (-)	-32.14%	8.35%	50.93%	49.09%	72.73%	61.14%
50-percentile UPTs (small cells)	Sch. A (Mbps)	Sch. B	Sch. C	Sch. D	Sch. E	Sch. F	Sch. F(b)
DL $\lambda^{DL}(u(q)) = 0.1$	17.70 (-)	45.81%	25.56%	60.28%	60.28%	60.28%	59.15%
DL $\lambda^{DL}(u(q)) = 0.3$	6.62 (-)	64.27%	86.00%	158.89%	157.23%	160.56%	157.23%
DL $\lambda^{DL}(u(q)) = 0.5$	3.17 (-)	63.06%	111.22%	195.31%	187.80%	201.15%	195.32%
UL $\lambda^{UL}(u(q)) = 0.1/2$	11.49 (-)	-23.01%	-0.57%	59.63%	61.11%	65.71%	60.37%
UL $\lambda^{UL}(u(q)) = 0.3/2$	9.98 (-)	-40.19%	-7.39%	29.56%	30.62%	43.47%	35.93%
UL $\lambda^{UL}(u(q)) = 0.5/2$	7.84 (-)	-54.34%	-16.87%	4.81%	4.38%	20.39%	12.55%
5-percentile UPTs (small cells)	Sch. A (Mbps)	Sch. B	Sch. C	Sch. D	Sch. E	Sch. F	Sch. F(b)
DL $\lambda^{DL}(u(q)) = 0.1$	7.28 (-)	58.61%	-12.36%	44.60%	45.31%	45.49%	44.28%
DL $\lambda^{DL}(u(q)) = 0.3$	1.10 (-)	56.61%	46.74%	208.88%	196.80%	209.30%	189.65%
DL $\lambda^{DL}(u(q)) = 0.5$	0.49 (-)	53.18%	66.79%	187.80%	176.36%	222.03%	215.88%
UL $\lambda^{UL}(u(q)) = 0.1/2$	6.76 (-)	-26.98%	-11.94%	44.27%	45.41%	48.40%	43.71%
UL $\lambda^{UL}(u(q)) = 0.3/2$	3.78 (-)	-38.84%	-6.66%	37.14%	38.71%	51.25%	34.63%
UL $\lambda^{UL}(u(q)) = 0.5/2$	2.05 (-)	-68.04%	-11.37%	-3.71%	-4.40%	31.14%	26.56%

As shown in Table V, it is easy to conclude that the straightforward dynamic TDD in the small-cell tier (Scheme B) leads to substantial performance degradation in the UL of

a HetNet, particularly for the macrocell tier, i.e., macrocell UL UPTs degradation of up to 88.27%. This is due to the significant intertier DL-to-UL interference, which indicates the

great difficulties in introducing dynamic TDD into HetNets if interlink interference is not properly managed. Similar observations were drawn for HomSCNs in Section VI. In contrast, Scheme B leads to performance gains in the DL of a HetNet, particularly for the small-cell tier because the scheduler favors the UL in the small-cell tier to combat the aforementioned strong intertier DL-to-UL interference; thus, the interference experienced by the DL transmissions in the small-cell tier is significantly reduced. However, the observed gains in the DL UPTs do not justify the use of Scheme B in a HetNet because the UL UPT reductions are enormous.

Let us now compare the baseline scheme (Scheme A) with the static TDD scheme with CRE and ABS operations (Scheme C). When the traffic load is low, e.g.,  $\lambda^{\text{DL}}(u(q)) = 0.1$ , the performance gains of Scheme C are low. This is because interference is not a severe problem; thus, the gain of eICIC is small or even negative. The 95-percentile macrocell DL UPT suffers from a loss of 10.79% because two subframes have been converted from DL to ABS, resulting in a moderate resource shortage. In contrast, when the traffic load is medium to high, e.g.,  $\lambda^{\text{DL}}(u(q)) \geq 0.3$ , in other words, when the interference is high, it can be seen that the performance gains of Scheme C are significant in almost all categories. The only exception is that the 50-percentile and the five-percentile UL UPTs of small-cell UEs suffer from a slight performance loss of 6.66%–16.87%. This negative impact is mostly caused due to the larger number of small-cell UEs to share the small-cell resources, as a result of macrocell offloading through range expansion. Having said that, it is important to notice that the 50-percentile and the five-percentile UL UPTs of all UEs together still rise by 121.28%–380.98%, indicating that CRE and eICIC benefit UL performance in general. This is because the random access network has been brought closer to small-cell ER UEs, thus greatly improving the qualities of ULs.

Regarding Scheme F, when the traffic load is low, e.g.,  $\lambda^{\text{DL}}(u(q)) = 0.1$ , the 95-percentile small-cell DL UPT and the 95-percentile small-cell UL UPT are basically contributed by cell-interior UEs. This is because these UEs suffer from low intercell interference, and the IC function is engaged to mitigate interlink interference. Moreover, when the traffic load is low, the coupling of DL scheduling and UL scheduling is quite weak. Hence, the UPT gains are mainly determined by the amount of additional transmission subframes in the DL or in the UL. Considering that, in dynamic TDD, the numbers of the available DL and UL subframes per ten subframes, respectively, increase from 7 to 9 and from 3 to 5, the UPT gains of Scheme F compared with Scheme C in terms of the 95-percentile small-cell DL UPT and the 95-percentile small-cell UL UPT should be around 2/7 and 3/5, respectively. The corresponding numerical results Table V confirm this observation, indicating 95-percentile small-cell DL UPT and the 95-percentile small-cell UL UPT gains around 26% $((1.7467-1.3884)/1.3884)$  and 63% $((1.8519-1.1381)/1.1381)$ , respectively. Note that such insightful observation cannot be obtained in our previous work [27] because of the nonideal link adaptor.

As can be further observed in Table V, compared with Scheme C, the proposed schemes (Schemes D, E, and F) achieve superior performances in all DL UPT categories. The

additional gains on top of those of Scheme C over Scheme A are particularly significant for the small-cell tier. To be more specific, additional gains of 35.83%(74.67%-38.84%)–55.55%(122.22%-66.67%), 34.72%(60.28%-25.56%)–89.93%(201.15%-111.22%), and 56.96%(44.60%-(-12.36%))–162.56%(209.30%-46.74%) can be observed in terms of 95-, 50- and five-percentile small-cell DL UPTs, respectively. The reason for these extra gains is that dynamic TDD is able to divert idle UL subframes for DL usage, thus boosting DL capacity. In the proposed scheduling policy, an ER UE may occupy as many as five dynamic TDD subframes for its DL transmission, thus greatly improving the five-percentile small-cell DL UPT.

As for the UL UPT, gains or losses maybe observed depending on the tier and the used scheme. When the traffic load is low to medium, e.g.,  $\lambda^{\text{DL}}(u(q)) \leq 0.3$ , the small-cell UL UPT performance of the proposed schemes (Schemes D, E, and F) improves. In more detail, extra performance gains of 52.70%(68.57%-15.87%)–75.35%(91.22%-15.87%), 36.95%(29.56%-(-7.39%))–66.28%(65.71%-(-0.57%)) and 43.80%(37.14%-(-6.66%))–60.34%(48.40%-(-11.94%)) are observed for the proposed schemes on top of those for Scheme C in terms of 95-, 50- and five-percentile small-cell UL UPTs, respectively. The story is different for the macrocell tier, when using Scheme D. In this case, macrocell UL UPTs suffer from a severe performance degradation as high as 79.87%, indicating that the intertier interlink interference from the small-cell DL is overwhelming for the macrocell UL. Thus, the intertier small-cell DL to macrocell UL IC is necessary for the macrocell UL to efficiently function if small-cell dynamic TDD operation is introduced into HetNets. When the traffic load is relatively high, e.g.,  $\lambda^{\text{DL}}(u(q)) = 0.5$ , the small-cell UL UPT performance of the proposed schemes (Schemes D and E) improves but not as much as with low to medium traffic loads. In more detail, extra performance gains of 40.74%(49.09%-8.35%), 21.68%(4.81%-(-16.87%)), and 7.66%(-3.71%-(-11.37%)) are observed for the proposed schemes (Schemes D and E) on top of those for Scheme C in terms of 95-, 50- and five-percentile UL UPTs, respectively. This shows that intertier IC is helpless in dealing with interlink interference inside the small-cell tier. In contrast, the proposed Scheme F with the required double IC, i.e., intertier small-cell DL to macrocell UL IC and DL-to-UL IC in the small-cell tier, considerably outperforms Scheme C, providing additional gains of 64.38%(72.73%-8.35%), 37.26%(20.39%-(-16.87%)) and 42.51%(31.14%-(-11.37%)) in terms of 95-, 50- and five-percentile UL UPTs, respectively. Double IC is thus necessary to aid the UL at high traffic loads.

It is important to note that the proposed partial IC scheme, i.e., Scheme F(b), turns out to be very efficient, resulting in small performance losses and low complexity compared with Scheme F (full IC). Therefore, we conclude that, for the used of dynamic TDD in HetNets, Scheme F(b) is a good choice, which strikes a beneficial balance between performance and complexity. Its nearly perfect score sheet is for two reasons: 1) The CRE, ABS, and small-cell DL to macrocell UL IC operations handle the intertier interference that paves the way for efficient dynamic TDD transmissions in the small-cell tier; and 2) the adaptive dynamic TDD transmission and the IC

operation to mitigate the small-cell DL to small-cell UL interference, together with the proposed scheduling policy in the small-cell tier, make the best of the transmission opportunities created by macrocell ABS and UL subframes. The only downside of Scheme F(b) is that the 95-percentile macrocell DL UPT suffers from a loss of 10.79% when  $\lambda^{\text{DL}}(u(q)) = 0.1$ . As explained earlier for Scheme D, this is because macrocells experience resource shortage when the traffic load is low due to the ABS operation of muting two subframes per ten subframes.

### VIII. COMPARISON OF DYNAMIC TIME DIVISION DUPLEX OPERATIONS IN HOMOGENEOUS SMALL-CELL NETWORKS AND HETEROGENEOUS NETWORKS

This paper is coherent for both HomSCNs and HetNets because 1) the optimization objectives are same for both network scenarios, 2) the additional complication of scheduler in HetNets compared with that in HomSCNs is removed by the ideal genie-aided LA mechanism, and 3) LTE-compliant DL/UL MIMO operations are considered for both network scenarios. Therefore, the performance results of HomSCNs and those of HetNets can be compared head to head; thus, we can draw some useful insights on the application of dynamic TDD in future networks as follows.

*Remark 1:* A higher flexibility of TDD configurations promises higher potential performance gains of dynamic TDD.

From Tables III and V, it can be observed that the performance gain of dynamic TDD is smaller in HetNets than that in HomSCNs, particularly in the UL. This is mainly because only limited flexibility of dynamic TDD can be achieved in HetNets due to the existence of ABSs and the restrictions it imposes on dynamic TDD transmissions. In more detail, in the HomSCNs, all subframes can be dynamic TDD subframes, and the DL-to-UL subframe ratio ranges from 2:3 (LTE Release 12) or 1:9 (LTE future releases) to 9:1, as discussed in Section VI. In contrast, in the HetNet small-cell tier, the DL-to-UL subframe ratio ranges from 5:5 to 9:1 since not all subframes can be dynamic TDD subframes, as discussed in Section VII. Hence, compared with dynamic TDD in HetNets, its counterpart in HomSCNs benefits from a much wider range of DL-to-UL subframe ratios, leading to larger performance gains due to the traffic-adaptive scheduling.

*Remark 2:* Interference mitigation is more crucial for the successful dynamic TDD operation in HetNets than in HomSCNs.

As shown in Tables III and V, we can conclude that interference mitigation is more crucial for the successful dynamic TDD operation in HetNets than that in HomSCNs. In more detail, the straightforward dynamic TDD operation is able to stand on its own with positive performance gains in HomSCNs (see Scheme 1 versus Scheme 3 in Table III), whereas the straightforward dynamic TDD operation suffers from huge performance losses in HetNets (see Scheme A versus Scheme B or Scheme C versus Scheme D in Table V), particularly in terms of the macrocell UL UPTs due to the devastating interference from small cell DL to macrocell UL. Hence, proper interference mitigation must be in place to handle the intertier interlink interference for dynamic TDD in HetNets.

*Remark 3:* Proper LA algorithms are essential for both HomSCNs and HetNets to reap the performance gains offered by dynamic TDD.

Comparing the results of a given dynamic TDD scheme in this paper and those in our previous work [24] and [27], we can find that some results in [24] and [27] were lack of insights and seemed counterintuitively small because a simple LA mechanism was assumed in our previous work; hence, the potential gains of dynamic TDD were not fully reaped. Such examples include Scheme 3 for the HomSCNs, as discussed in Section VI, and Scheme B for the HetNets, as discussed in Section VII. Therefore, it is very important for dynamic TDD networks, both HomSCNs and HetNets, to have proper LA algorithms to predict the drastic interference fluctuation due to the dynamic and nonuniform TDD configurations in neighboring cells.

### IX. CONCLUSION

In this paper, using a unified framework, we present new results on dynamic TDD transmissions in both HomSCNs and HetNets, and we draw the following conclusions.

- The dynamic TDD with (partial) IC is shown to provide large gains, particularly in terms of the five-percentile UL UPT, when the traffic load is medium to relatively high.
- The combination of CC and IC, with or without ULPB, is not an efficient strategy because the CC scheme and IC scheme are somehow redundant.
- The combination of CC and ULPB is recommended for low-complexity implementation, whereas that of ULPB and IC can bring much more performance gains at the expense of higher complexity.

In our study on dynamic TDD in HetNets, we show that to make dynamic TDD operate properly in HetNets, we have the following.

- Small-cell DL to macrocell UL IC is indispensable for the macrocells to achieve reasonable UL UPTs.
- Another DL-to-UL IC in the small-cell tier is required to mitigate the interlink interference among small cells, particularly when the traffic load is medium or high.
- The proposed BOIC scheme results in small performance losses and low complexity compared with the full IC scheme, making it a good choice for practical use.

To improve the feasibility and the generality of the proposed algorithms, as future work, we will consider more practical assumptions in this paper such as errors in buffer size, investigate practical LA algorithms and more practical non-IC receivers, and use theories such as machine learning techniques, game theory, distributed optimization, etc., to design low-complexity algorithms, particularly for dynamic TDD in HetNets.

### ACKNOWLEDGMENT

The authors would like to thank all the anonymous reviewers for their helpful comments and constructive suggestions to improve early drafts of this paper.

## REFERENCES

- [1] "Cisco visual networking index: Global mobile data traffic fore-cast update," Cisco, San Francisco, CA, USA, 2011–2016, Feb. 2012.
- [2] S. Sesia, I. Toufik, and M. Baker, *LTE: The UMTS Long Term Evolution*, 2nd ed. New York, NY, USA: Wiley, 2011.
- [3] D. López-Pérez, M. Ding, H. Claussen, and A. Jafari, "Towards 1 Gbps/UE in cellular systems: Understanding ultra-dense small cell deployments," *IEEE Commun. Surveys Tuts.*, vol. 17, no. 4, pp. 2078–2101, Jun. 2015.
- [4] "Draft report of 3GPP TSG RAN meeting #66," ETSI MCC, Third-Generation Partnership Project, Sophia Antipolis Cedex, France, Dec. 2014.
- [5] H. Zhang, C. Jiang, J. Cheng, and V. C. M. Leung, "Cooperative interference mitigation and handover management for heterogeneous cloud small cell networks," *IEEE Mag. Wireless Commun.*, vol. 22, no. 3, pp. 92–99, Jun. 2015.
- [6] H. Zhang, X. Chu, W. Guo, and S. Wang, "Coexistence of Wi-Fi and heterogeneous small cell networks sharing unlicensed spectrum," *IEEE Commun. Mag.*, vol. 53, no. 3, pp. 158–164, Mar. 2015.
- [7] Z. Luo, M. Ding, and H. Luo, "CC on/off scheduling using learning-based prediction for LTE in the unlicensed spectrum," *IEEE Commun. Lett.*, vol. 19, no. 12, pp. 2158–2161, Dec. 2015.
- [8] Y. Qin, M. Ding, M. Zhang, H. Yu, and H. Luo, "Relaying robust beamforming for device-to-device communication with channel uncertainty," *IEEE Commun. Lett.*, vol. 18, no. 10, pp. 1859–1862, Oct. 2014.
- [9] Y. Niu *et al.*, "Exploiting device-to-device communications in joint scheduling of access and backhaul for mmWave small cells," *IEEE J. Sel. Areas Commun.*, vol. 33, no. 10, pp. 2052–2069, Oct. 2015.
- [10] H. Zhang *et al.*, "Resource allocation for cognitive small cell networks: A cooperative bargaining game theoretic approach," *IEEE Trans. Wireless Commun.*, vol. 14, no. 6, pp. 3481–3493, Jun. 2015.
- [11] H. Zhang, C. Jiang, X. Mao, and H. Chen, "Interference-limited resource optimization in cognitive femtocells with fairness and imperfect spectrum sensing," *IEEE Trans. Veh. Technol.*, vol. 65, no. 3, pp. 1761–1771, Mar. 2016.
- [12] H. Zhang *et al.*, "Resource allocation in spectrum-sharing OFDMA femtocells with heterogeneous services," *IEEE Trans. Commun.*, vol. 62, no. 7, pp. 2366–2377, Jul. 2014.
- [13] D. López-Pérez, X. Chu, A. V. Vasilakos, and H. Claussen, "On distributed and coordinated resource allocation for interference mitigation in self-organizing LTE networks," *IEEE/ACM Trans. Netw.*, vol. 21, no. 4, pp. 1145–1158, Aug. 2013.
- [14] D. López-Pérez, X. Chu, A. V. Vasilakos, and H. Claussen, "Power minimization based resource allocation for interference mitigation in OFDMA femtocell networks," *IEEE J. Sel. Areas Commun.*, vol. 32, no. 2, pp. 333–344, Feb. 2014.
- [15] J. G. Andrews, "Seven ways that HetNets are a cellular paradigm shift," *IEEE Commun. Mag.*, vol. 51, no. 3, pp. 136–144, Mar. 2013.
- [16] D. López-Pérez *et al.*, "Enhanced inter-cell interference coordination challenges in heterogeneous networks," *IEEE Wireless Commun. Mag.*, vol. 18, no. 3, pp. 22–30, Jun. 2011.
- [17] D. López-Pérez, C. Xiaoli, and I. Guvenc, "On the expanded region of picocells in heterogeneous networks," *IEEE Sel. Topics Signal Process.*, vol. 6, no. 3, pp. 281–294, Jun. 2012.
- [18] M. Ding, D. López-Pérez, G. Mao, P. Wang, and Z. Lin, "Will the area spectral efficiency monotonically grow as small cells go dense?" in *Proc. IEEE Globecom*, arXiv: 1505.01920 [cs.NI], Dec. 2015.
- [19] M. Ding, P. Wang, D. López-Pérez, G. Mao, and Z. Lin, "Performance impact of LoS and NLoS transmissions in dense cellular networks," *IEEE Trans. Wireless Commun.*, vol. 15, no. 3, pp. 2365–2380, Mar. 2016.
- [20] M. Ding, D. López-Pérez, G. Mao, and Z. Lin, "DNA-GA: A new approach of network performance analysis," *Proc. IEEE ICC 2016*, arXiv:1512.05429 [cs.IT], to be published.
- [21] "Physical layer procedures (Release 11)," Third-Generation Partnership Project, Sophia Antipolis Cedex, France, TS 36.213 V11.3.0, Jun. 2013.
- [22] I. Chih-Lin *et al.*, "Toward green and soft: A 5G perspective," *IEEE Commun. Mag.*, vol. 52, no. 2, pp. 66–73, Feb. 2014.
- [23] Z. Shen, A. Khoryaev, E. Eriksson, and X. Pan, "Dynamic uplink-downlink configuration and interference management in TD-LTE," *IEEE Commun. Mag.*, vol. 50, no. 11, pp. 51–59, Nov. 2012.
- [24] M. Ding, D. López-Pérez, A. V. Vasilakos, and W. Chen, "Dynamic TDD transmissions in homogeneous small cell networks," in *Proc. IEEE ICC*, Jun. 2014, pp. 616–621.
- [25] S. Song, Y. Chang, H. Xu, D. Zheng, and D. Yang, "Energy efficiency model based on stochastic geometry in dynamic TDD cellular networks," in *Proc. IEEE ICC*, Jun. 2014, pp. 889–894.
- [26] "Further enhancements to LTE Time Division Duplex (TDD) for Downlink-Uplink (DL-UL) interference management and traffic adaptation (Release 11)," Third-Generation Partnership Project, Sophia Antipolis Cedex, France, TR 36.828 V11.0.0, Jun. 2012.
- [27] M. Ding, D. López-Pérez, R. Xue, A. V. Vasilakos, and W. Chen, "Small cell dynamic TDD transmissions in heterogeneous networks," in *Proc. IEEE ICC*, Jun. 2014, pp. 4881–4887.
- [28] "R1-132350: DL power control based interference mitigation for eIMTA," Sharp, Fukuoka, Japan, 3GPP RAN1 Meet. #73, May 2013.
- [29] "R1-132351: UL power control based interference mitigation for eIMTA," Sharp, Fukuoka, Japan, 3GPP RAN1 Meet. #73, May 2013.
- [30] A. Galindo-Serrano and L. Giupponi, "Distributed Q-learning for aggregated interference control in cognitive radio networks," *IEEE Trans. Veh. Technol.*, vol. 59, no. 4, pp. 1823–1834, May 2010.
- [31] L. Giupponi, A. Galindo-Serrano, P. Blasco, and M. Dohler, "Dognitive networks: An emerging paradigm for dynamic spectrum management [Dynamic Spectrum Management]," *IEEE Trans. Wireless Commun.*, vol. 17, no. 4, pp. 47–54, Aug. 2010.
- [32] "R1-132304: Enhanced fast ABS adaptation for Rel-12 small cell scenario 1," Nokia Siemens Netw., Nokia, Fukuoka, Japan, 3GPP RAN1 Meet. #73, May 2013.
- [33] D. López-Pérez and H. Claussen, "Duty cycles and load balancing in HetNets with eCIC almost blank subframes," in *Proc. IEEE PIMRC*, London, U.K., Sep. 2013, pp. 1–6.
- [34] [Online]. Available: <http://wnt.sjtu.edu.cn/flint/html/index.html>
- [35] "Further advancements for E-UTRA physical layer aspects (Release 9)," Third-Generation Partnership Project, Sophia Antipolis Cedex, France, TR 36.814 V9.0.0, Mar. 2010.
- [36] "Base Station (BS) radio transmission and reception," Third-Generation Partnership Project, Sophia Antipolis Cedex, France, TS 36.104 V11.4.0, Mar. 2013.



**Ming Ding** (M'12) received the B.S. and M.S. (with first-class honors) degrees in electronics engineering and the Ph.D. degree in signal and information processing from Shanghai Jiao Tong University (SJTU), Shanghai, China, in 2004, 2007, and 2011, respectively.

From September 2007 to September 2011, during his doctoral studies, he was also a Researcher/Senior Researcher with Sharp Laboratories, China (SLC). After receiving the Ph.D. degree, he continued working with SLC as a Senior Researcher/Principal Researcher until September 2014, when he joined the National Information and Communications Technology Australia (NICTA). In September 2015, Commonwealth Scientific and Industrial Research Organization (CSIRO) and NICTA joined forces to create Data 61, where he continued his research in this new R&D center. He has been working on beyond third-generation (B3G), fourth-generation (4G), and fifth-generation (5G) wireless communication networks for more than nine years. In addition, he served as the Algorithm Design Director and Programming Director for a system-level simulator of future telecommunication networks in SLC for more than seven years. His research interests include synchronization, multiple-input–multiple-output technology, cooperative communications, heterogeneous networks, device-to-device communications, and modeling of wireless communication systems. He has authored more than 30 papers in IEEE journals and conferences, all in recognized venues, and about 20 3GPP standardization contributions, as well as a Springer book entitled *Multi-point Cooperative Communication Systems: Theory and Applications*. In addition, as the first inventor, he holds 15 Chinese, seven Japanese, three U.S., two Korean patents, and he has co-authored another 100+ patent applications on 4G/5G technologies.

Dr. Ding has served as a Guest Editor, a Co-Chair, and Technical Program Committee member of several IEEE top-tier journals and conferences, e.g., the IEEE JOURNAL ON SELECTED AREAS ON COMMUNICATIONS, IEEE COMMUNICATIONS MAGAZINE, and IEEE Global Communications Conference Workshops. He received the President's Award of SLC in 2012. He served as one of the key members in the 4G/5G standardization team when it was awarded the Sharp Company Best Team: LTE Standardization Patent Portfolio, in 2014.



**David López-Pérez** (M'12) received the Ph.D. degree in wireless networking from the University of Bedfordshire, Bedfordshire, U.K. in 2011.

From February 2005 to February 2006, he was with Vodafone, Spain, working in the area of network planning and optimization. In 2009, he was an Invited Researcher with CITI INSA, France, and in 2011, with DOCOMO USA Labs, CA, USA. From August 2010 to December 2011, he was a Research Associate with King's College London, London, U.K., carrying out postdoctoral studies. He is currently a Member of the Technical Staff with Bell Laboratories, Alcatel-Lucent, Dublin, Ireland. He was the Editor of *Heterogeneous Cellular Networks: Theory, Simulation and Deployment* (Cambridge University Press, 2012) and has published more than 70 book chapters, journal, and conference papers, all in recognized venues, and has filed more than 30 patents applications. His main research interests include heterogeneous networks, small cells, interference and mobility management, and network optimization and simulation.

Dr. López-Pérez has served as a Guest Editor for a number of journals, such as the IEEE JOURNAL ON SELECTED AREAS ON COMMUNICATIONS and IEEE COMMUNICATIONS MAGAZINE, as a Technical Program Committee Member of top-tier conferences, such as the IEEE Global Communications Conference and the IEEE International Conference on Communications, and as a Cochair of a number of workshops. He has received both the Bell Labs Alcatel-Lucent Award of Excellence and Certificate of Outstanding Achievement for his publications and patent contributions. He was a Finalist for the Scientist of the Year Prize in The Irish Laboratory Awards in 2013. He was appointed Ph.D. Marie-Curie Fellow in 2007 and Exemplary Reviewer for IEEE COMMUNICATIONS LETTERS in 2011.

Dr. López-Pérez has served as a Guest Editor for a number of journals, such as the IEEE JOURNAL ON SELECTED AREAS ON COMMUNICATIONS and IEEE COMMUNICATIONS MAGAZINE, as a Technical Program Committee Member of top-tier conferences, such as the IEEE Global Communications Conference and the IEEE International Conference on Communications, and as a Cochair of a number of workshops. He has received both the Bell Labs Alcatel-Lucent Award of Excellence and Certificate of Outstanding Achievement for his publications and patent contributions. He was a Finalist for the Scientist of the Year Prize in The Irish Laboratory Awards in 2013. He was appointed Ph.D. Marie-Curie Fellow in 2007 and Exemplary Reviewer for IEEE COMMUNICATIONS LETTERS in 2011.



**Ruiqi Xue** received the B.S. and M.S. degrees in electronics engineering from Shanghai Jiao Tong University, Shanghai, China, in 2012 and 2015, respectively.

He is familiar with the modeling of wireless communication systems and has published several related papers and patents. His main research interests include multiple-input-multiple-output technology, heterogeneous networks, and interference mitigation.



**Athanasios V. Vasilakos** (M'00-SM'11) is currently a Professor with Lulea University of Technology, Luleå, Sweden.

Mr. Vasilakos serves as the General Chair of the European Alliances for Innovation. He served or is serving as an Editor for many technical journals, such as the IEEE TRANSACTIONS ON NETWORK AND SERVICE MANAGEMENT, the IEEE TRANSACTIONS ON CLOUD COMPUTING, the IEEE TRANSACTIONS ON INFORMATION FORENSICS AND SECURITY, the IEEE TRANSACTIONS ON CYBERNETICS, the IEEE TRANSACTIONS ON NANOBIOSCIENCE, the IEEE TRANSACTIONS ON INFORMATION TECHNOLOGY IN BIOMEDICINE, the *ACM Transactions on Autonomous and Adaptive Systems*, and the IEEE JOURNAL ON SELECTED AREAS ON COMMUNICATIONS.

Mr. Vasilakos serves as the General Chair of the European Alliances for Innovation. He served or is serving as an Editor for many technical journals, such as the IEEE TRANSACTIONS ON NETWORK AND SERVICE MANAGEMENT, the IEEE TRANSACTIONS ON CLOUD COMPUTING, the IEEE TRANSACTIONS ON INFORMATION FORENSICS AND SECURITY, the IEEE TRANSACTIONS ON CYBERNETICS, the IEEE TRANSACTIONS ON NANOBIOSCIENCE, the IEEE TRANSACTIONS ON INFORMATION TECHNOLOGY IN BIOMEDICINE, the *ACM Transactions on Autonomous and Adaptive Systems*, and the IEEE JOURNAL ON SELECTED AREAS ON COMMUNICATIONS.



**Wen Chen** (M'03-SM'11) received the B.S. and M.S. degrees from Wuhan University, Wuhan, China, in 1990 and 1993, respectively, and the Ph.D. degree from The University of Electro-Communications, Tokyo, Japan, in 1999.

From 1999 to 2001, he was a Researcher with the Japan Society for the Promotion of Sciences. In 2001, he joined the University of Alberta, Edmonton, AB, Canada, starting as a Postdoctoral Fellow with the Information Research Laboratory and continuing as a Research Associate with the Department of

Electrical and Computer Engineering. Since 2006, he has been a Full Professor with the Department of Electronic Engineering, Shanghai Jiao Tong University, Shanghai, China, where he is also the Director of the Institute for Signal Processing and Systems. Since 2014, he has been the Dean of electronic engineering and automation with Guilin University of Electronic Technology, Guilin, China. He is the author of more than 70 papers in IEEE JOURNALS AND TRANSACTIONS and more than 100 papers in IEEE conference publications. His research interests include network coding, cooperative communications, cognitive radio, and multiple-input-multiple-output orthogonal frequency-division systems.